CT of Postoperative Repair of the Ascending Aorta and Aortic Arch

Kaitlin M. Marquis, MD
Muhammad Naeem, MBBS
Mohamed Zak Rajput, MD
Demetrios A. Raptis, MD
Kacie L. Steinbrecher, MD
J. Westley Ohman, MD
Sanjeev Bhalla, MD
Constantine A. Raptis, MD

Abbreviation: MIP = maximum intensity projection

RadioGraphics 2021; 41:1300–1320

https://doi.org/10.1148/rg.2021210026

Content Codes: CH CT IR VA

From the Mallinckrodt Institute of Radiology (K.M.M., M.N., M.Z.R., D.A.R., K.L.S., S.B., C.A.R.) and Department of Surgery (J.W.O.), Washington University School of Medicine, 510 S Kingshighway Blvd, St Louis, MO 63110. Presented as an education exhibit at the 2020 RSNA Annual Meeting. Received February 9, 2021; revision requested March 9 and received April 11; accepted April 20. For this journal-based SA-CME activity, the authors, editor, and reviewers have disclosed no relevant relationships. **Address correspondence to** K.M.M. (e-mail: *kmarquis@wustl.edu*).

SA-CME LEARNING OBJECTIVES

After completing this journal-based SA-CME activity, participants will be able to:

- Recognize the imaging appearances of the most used components of thoracic aorta repairs.
- Characterize repairs of the ascending aorta.
- Understand the appearances of aortic arch repairs.

See rsna.org/learning-center-rg.

While many of the classic open surgical repairs are still used to repair the ascending aorta, management of the aortic arch has become more complex via implementation of newer open surgical and endovascular techniques. Furthermore, techniques are often combined in novel repairs or to allow extended anatomic coverage. As such, a framework that rests on understanding the expected postoperative appearance is necessary for the diagnostic radiologist to best interpret CT studies in these patients. After reviewing the imaging appearances of the common components used in proximal aortic repair, the authors present a structured approach that focuses on the key relevant questions that diagnostic radiologists should consider when interpreting CT studies in these patients. For repair of the ascending aorta, this includes determining whether the aortic valve has been repaired, whether the sinuses of Valsalva have been repaired, and how the coronary arteries were managed, when necessary. In repairs that involve the aortic arch, the relevant considerations relate to management of the arch vessels and the distal extent of the repair. In focusing on these questions, the diagnostic radiologist will be able to identify and describe the vast majority of repairs. Understanding these questions will also facilitate improved understanding of novel repairs, which often use these basic building blocks. Finally, complications—which typically involve infection, noninfectious repair breakdown, hemorrhage, problems with endografts, or disease of the remaining adjacent aorta—will be identifiable as deviations from the expected postoperative appearance.

Online supplemental material is available for this article.

Introduction

Over the past several decades, techniques for repair of the ascending aorta and aortic arch (proximal aortic repair) have evolved and become increasingly complex and diversified. Many of the classic repair techniques are still used, although they are continually modified, improved on, and used in conjunction with newer techniques and devices to produce novel repairs. Patients treated with these procedures will inevitably undergo CT as part of routine follow-up and evaluation for suspected complications. As such, the diagnostic radiologist has a pivotal role in postoperative evaluation and management of patients who have undergone proximal aortic repair.

As with all patients who have undergone a surgical procedure, interpretation of these studies requires a fundamental understanding of the expected postoperative appearance. This begins with recognizing the imaging appearance of the most used components—or "nuts and bolts"—of proximal aortic repairs. From there, an organized

TEACHING POINTS

- At CT, when the vessel a felt ring encircles is viewed along its long axis, the felt ring will appear as focal small hyperattenuating structures along its periphery. If an orthogonal plane or volume-rendered image is created perpendicular to the vessel at the level of the felt ring, the ring nature of this reinforcement will be confirmed. Identifying felt rings is helpful in determining the extent of open grafts, given that they are frequently used to reinforce anastomoses.
- At CT, patients who have undergone composite graft aortic replacement have findings of a graft that begins at the valve plane and extends cranially. These grafts are typically tubular and may have folds or bends in them to accommodate their course in the mediastinum. When felt rings are used, there will be only a distal felt ring, which allows distinction of a composite graft from a supracoronary graft. The normal anatomy of the sinuses of Valsalva will be absent, and the coronary arteries will be anastomosed.
- When the coronary artery harvested with the modified Bentall technique is reimplanted on the aorta, postoperative CT will demonstrate the larger trumpetlike origin, which is typically reinforced with surrounding felt after it is sutured to produce what is termed a *coronary button*.
- In endovascular repairs, the arch vessels may be managed using the chimney or snorkel technique, in which stent-grafts are deployed within the arch vessels that then run alongside an endovascular graft deployed in the aortic arch. Some endovascular stent-grafts specifically designed for the aortic arch have fenestrae or uncovered portions that communicate with the arch vessels or allow deployment of stents from the arch vessels into the lumen of the endovascular graft.
- In all elephant trunk variations, the CT appearance will be similar, with *(a)* findings of open surgical repair of the proximal aorta with managed arch vessels (island, debranching, or four-branched surgical graft) and *(b)* an endovascular stent extending into the distal aspect of the open graft.

assessment that focuses on key questions can be used to characterize repairs of the ascending aorta and aortic arch. Once the expected postoperative appearance of repairs of the ascending aorta and aortic arch is understood, unexpected imaging findings concerning for complications will be identifiable.

Nuts and Bolts

Surgical Grafts

Grafts used in open surgical proximal thoracic aorta repairs are typically made of synthetic polyethylene (Dacron; DuPont) (1–3). Rarely, aortic homografts procured from a human donor are used; this is uncommon given the increased complexity of these operations and the frequent failure of these types of grafts (4–7). Grafts can be used to replace aortic tissue only or be fashioned directly into a valvular prosthesis, which may be mechanical or bioprosthetic. A surgical graft fashioned into a valvular prosthesis is termed a *composite graft* (1).

Synthetic aortic grafts can be identified at noncontrast CT by their hyperattenuating appearance in comparison with the native aorta, a finding that may be difficult to perceive at postcontrast imaging owing to the adjacent blood pool (Fig 1). Potential mimics of a hyperattenuating surgical graft include *(a)* circumferential calcification and *(b)* relative hyperattenuation of the wall in comparison with the blood pool in patients with anemia.

Aortic grafts can also be identified by their nonanatomic appearance. Grafts are less pliable than the native aorta and—instead of having a smoothly curved morphology—typically have a straighter configuration with accompanied angulations. As such, they are often more redundant than would be expected of the native aorta and may even produce folds. Identifying graft folds is important because when viewed only on axial images, they may simulate an intimomedial flap (8) (Fig 2).

Aortic grafts also lack normal anatomic landmarks. This is particularly relevant in identifying aortic root repairs, as almost all grafts that extend to the aortic valve plane will be straight and not demonstrate the waist of the sinotubular junction or normal sinuses of Valsalva. Additionally, subtle caliber changes at the interface with the native aorta and the presence of reinforcement material can be used to define the extent of aortic grafts. Multiplanar reconstructions are useful in characterizing the nonanatomic nature of grafts by depicting their extent, the presence of folds, and the absence of normal anatomic landmarks.

Open surgical aortic repair can be performed with the inclusion technique or interposition technique. The inclusion technique, originally described by Bentall and De Bono (9), was introduced as a method to control bleeding and prevent graft leaking. In this technique, the native aorta is incised and then sutured around the graft, creating a potential space between the native aorta and the graft material. Accumulation of blood or fluid in the perigraft space can have the unintended consequence of producing tension on the anastomosis, thereby increasing the risk of pseudoaneurysm formation (10). At CT, this potential space may not normally be visible, but if the native aorta was calcified, it may be seen surrounding the graft itself (Fig 3).

With advancements in graft technology and surgical technique, the inclusion technique has largely been replaced by the interposition technique, in which the diseased aorta is excised and replaced with an interposition graft. Despite the lack of a surgically created potential space—as seen with the inclusion technique—interposition grafts may also have a potential space surrounding them owing to the presence of residual aortic

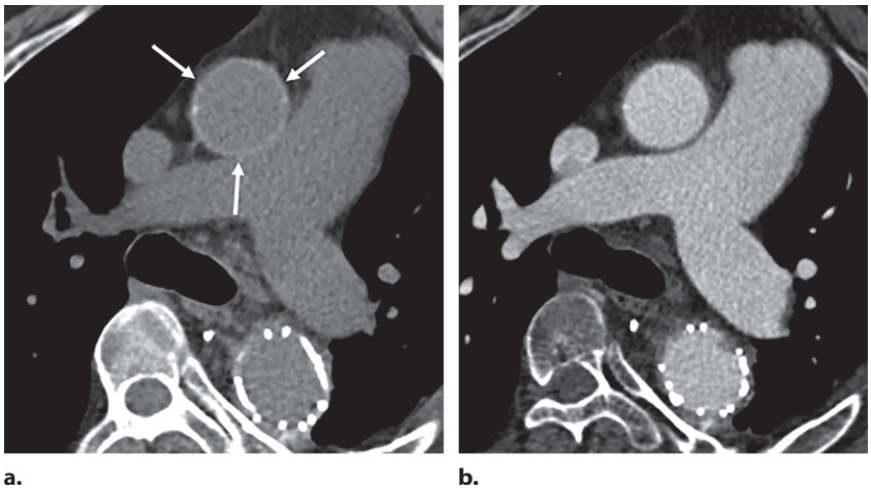

Figure 1. Elephant trunk repair in a 24-year-old man. The repair was performed with a Dacron graft (DuPont) replacing the ascending aorta and an endovascular stent in the descending aorta. **(a)** Axial noncontrast CT image shows that the graft has a mildly hyperattenuating wall (arrows). **(b)** On a corresponding contrast-enhanced image, the graft is not identifiable.

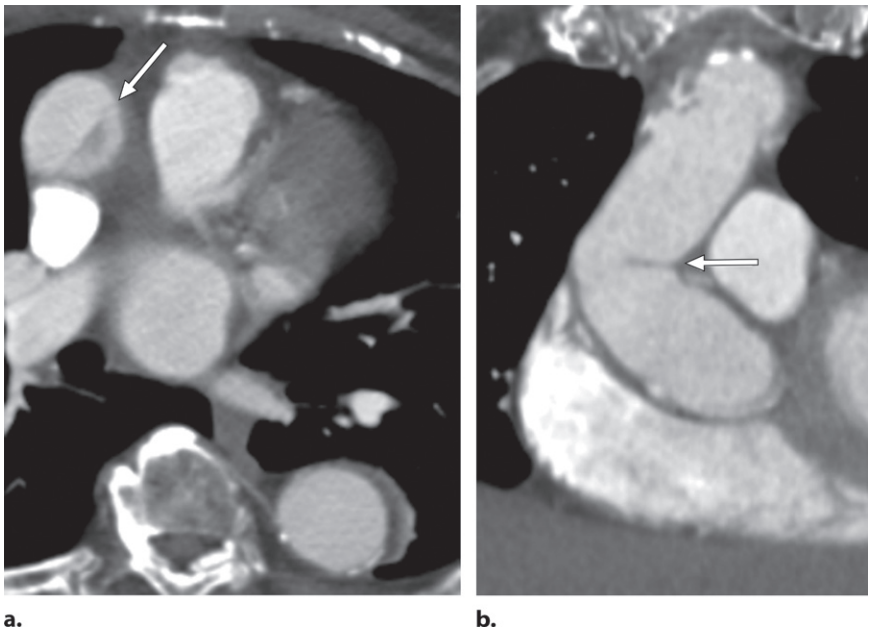

Figure 2. Synthetic graft fold in a 71-year-old man with an open surgical graft of the ascending aorta. **(a)** Axial CT image shows a linear area of hypoattenuation (arrow) in the ascending aortic portion of the graft. **(b)** Oblique multiplanar reconstruction shows that the finding in **a** is a fold (arrow) due to redundancy in the graft. Intimomedial flaps do not occur in an open graft because it is a synthetic tube and not native aorta. Open grafts have a straighter and more angulated morphology than that of the native aorta; this morphology can produce folds that simulate intimomedial flaps.

tissue, adhesions, or resolved hematoma. On occasion, this material can calcify and be detectable at CT (2,11,12).

In addition to being used in repair of the thoracic aorta, synthetic vascular grafts can also be used to reconstruct the arch vessels. Grafts used to reconstruct the arch vessels can be individual or have multiple limbs with joined proximal portions that attach to the aorta. Carotid-carotid and left carotid-subclavian grafts can also be fashioned to connect the arch vessels to each other in a sequential or "daisy chain" configuration (13).

When used in conjunction with an endovascular thoracic aorta stent, left carotid-subclavian grafts are often accompanied by occlusion of the proximal left subclavian artery origin to prevent endoleaks. Occlusion of the left subclavian artery can be performed surgically but is more often accomplished with an endovascular approach via placement of vascular occluders and plugs (14–16). Occluding devices are easily identifiable at CT as disk- or dumbbell-shaped hyperattenuating structures that work by promoting thrombogenesis (Fig 4).

Aside from being used in primary vascular repair, short side grafts are often used for purposes of cardiopulmonary bypass cannulation. These grafts can be fastened to the aorta or, when the aorta is not suitable, to more peripheral vessels such as the axillary, innominate, or subclavian artery. In some cases, an ascending aortic graft may have a small side branch for vascular access built into it that can be used for cardiopulmonary bypass after the distal anastomosis is complete.

At postrepair imaging, side-branch grafts can have variable configurations. Their distal margins can be tapered or square, and there is often

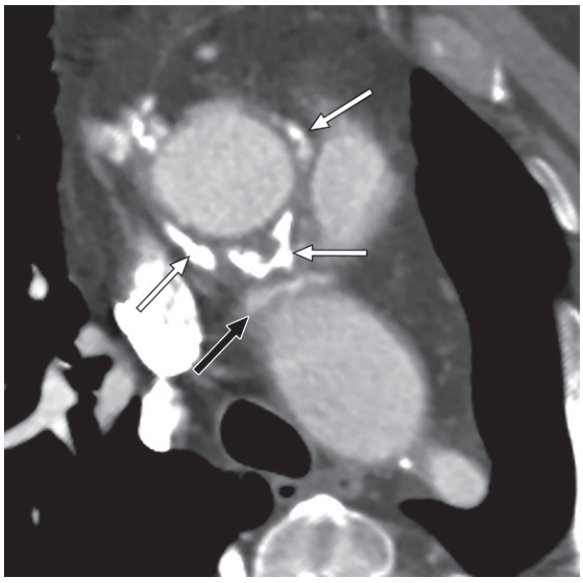

Figure 3. Axial CT image shows a composite graft repair of the ascending aorta using the inclusion technique. Calcified material surrounding the graft (white arrows) corresponds to the native inclusion aorta wrapped around the graft. Note the felt reinforcement (black arrow), which is partially included along the undersurface of the aortic arch.

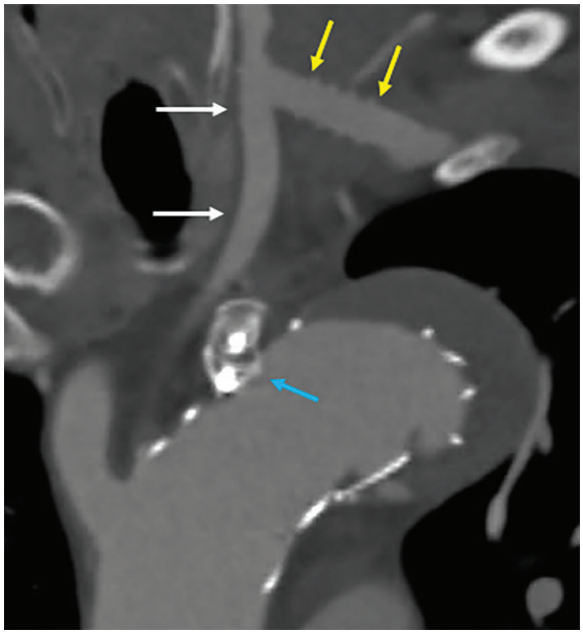

Figure 4. Oblique coronal maximum intensity projection (MIP) CT reconstruction in a patient with an endovascular stent-graft across the subclavian artery origin. To prevent back filling of the excluded aorta, an occluder device (blue arrow) was placed at the origin of the left subclavian artery. The left subclavian artery was revascularized using a surgical graft (yellow arrows) from the left common carotid artery (white arrows). The surgical graft can be identified by its regularly repeating folds.

suture material, felt, or clips at their apex to close them. Knowledge of the imaging appearance of side-branch grafts is essential to prevent misidentification as a pseudoaneurysm (17) (Fig 5).

Reinforcements: Felt Rings, Pledgets, Sutures, and Clips

Felt rings and pledgets, typically made of tetrafluoroethylene, are used to seal and reinforce potential points of failure, which include vascular access sites and anastomoses between the graft and native aortic tissue. Felt rings and pledgets are readily identifiable as hyperattenuating structures at both noncontrast and contrast-enhanced CT. As would be inferred from their name, felt rings are linear structures that can be used to encircle the aorta and are of particular value in reinforcing suture lines. At CT, when the vessel a felt ring encircles is viewed along its long axis, the felt ring will appear as focal small hyperattenuating structures along its periphery. If an orthogonal plane or volume-rendered image is created perpendicular to the vessel at the level of the felt ring, the ring nature of this reinforcement will be confirmed. Identifying felt rings is helpful in determining the extent of open grafts, given that they are frequently used to reinforce anastomoses (2,3) (Fig 6).

Felt pledgets are used primarily to reinforce vascular access sites and—like felt rings—appear at CT as small round or oblong hyperattenuating structures. They are typically positioned along the ascending aorta or major branch vessels, either directly apposed to the outer wall of the aorta or at the tip of side-branch grafts used for cannulation (Fig 7). Felt can also be used to reinforce other access sites, including those used for left ventricle or pulmonary vein cannulation (2,3,17).

Surgical sutures are often used to reinforce vascular access sites, side-branch grafts, and anastomoses and appear at CT as thin hyperattenuating linear structures. Sutures can also be fastened to suture anchors. Recognizing suture anchors, which are most often small hook-shaped linear structures, can be particularly helpful in detecting the presence of a bioprosthetic aortic valve replacement, as the leaflets themselves will not be identifiable, since they are native human tissue. In addition, some surgeons may use metallic automated "suture fasteners" such as the Cor-Knot (LSI Solutions) to secure valvular anastomoses; at CT, these appear as foci of metallic attenuation along the rim of a valvular anastomosis (Fig 8).

Surgical clips are of varying sizes but are typically made of metal. As such, they are very hyperattenuating at CT. They appear as straight and well-marginated hyperattenuating structures that can produce some beam-hardening artifact and are often thicker and straighter than sutures. Surgical clips have various purposes in thoracic aorta repair, including occluding vessels for hemostasis and closing side-branch grafts used for cannulation.

When a question arises as to whether a high-attenuation finding at CT represents one of

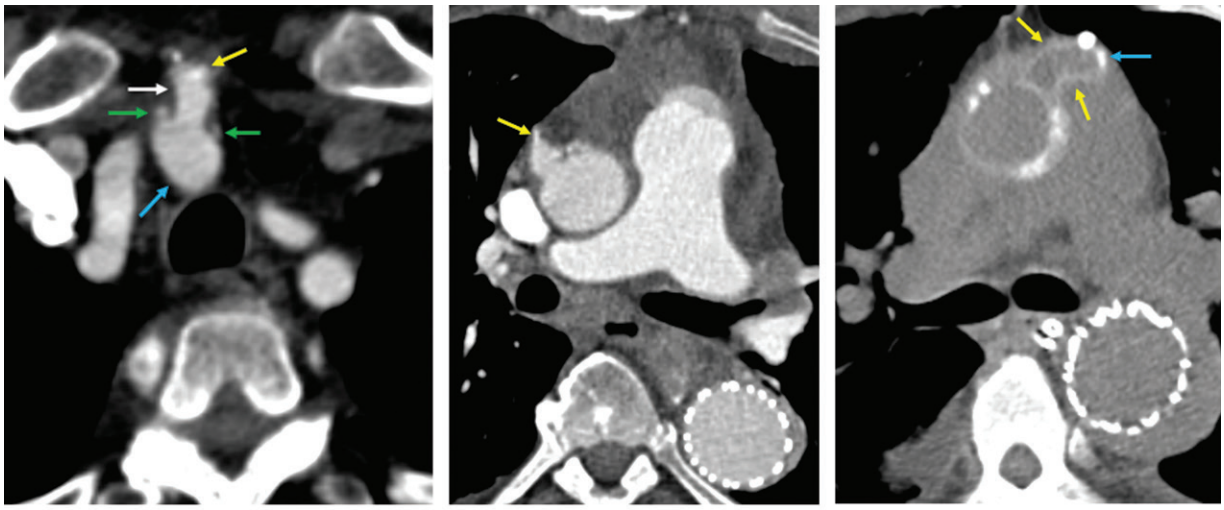

Figure 5. Cannulation sites. **(a)** Side-branch graft in a 67-year-old woman after supracoronary aortic repair for dissection (not shown). Axial CT image shows a squared-off side-branch graft (white arrow) from the innominate artery (blue arrow). A felt pledget is seen at the tip (yellow arrow); there is also felt reinforcement (green arrows) at the junction with the innominate artery. **(b)** Cannulation graft in a 65-year-old man after proximal aortic repair. Axial CT image shows a tapered cannulation graft along the right anterolateral aorta with a hyperattenuating suture at its apex (arrow). **(c)** Side-branch graft in a 70-year-old man after proximal aortic repair. Axial noncontrast CT image shows the hyperattenuating wall (yellow arrows) of a side-branch graft used to cannulate the aorta for bypass. The end of the side graft has a small amount of felt at its tip (blue arrow).

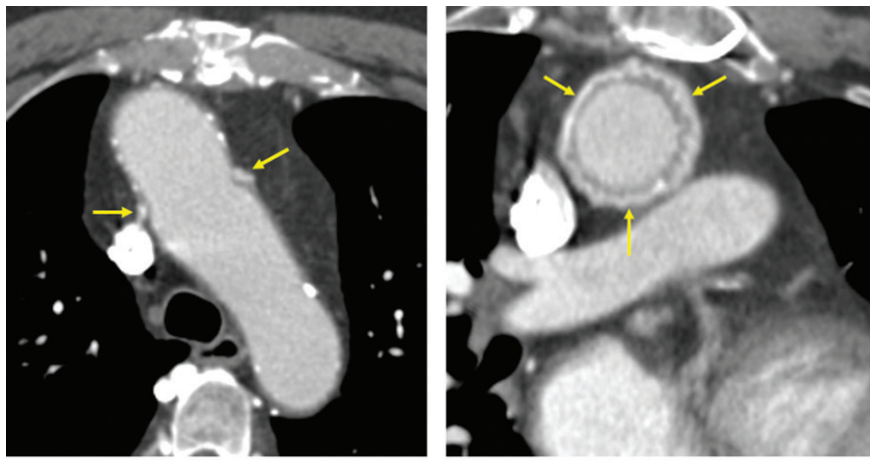

Figure 6. Felt ring in a 65-year-old man after proximal aortic repair. **(a)** Axial CT image shows hyperattenuating structures (arrows) along the wall of the aorta. **(b)** Perpendicular-plane CT image through these structures shows that they represent a circumferential felt ring (arrows). Felt rings are used to reinforce anastomoses; therefore, identifying them can help define the margins of a surgical graft.

the described reinforcement materials, blood, extravasated contrast material, or a pseudoaneurysm, comparison with prior studies or performing a noncontrast examination can be crucial for definitive identification. In addition, careful review of operative notes may be helpful for determining the intended placement of reinforcement materials.

Endovascular Stent-Grafts

Endovascular stent-grafts are composed of an inner metallic skeleton often made of nitinol, which is readily identifiable at CT with hyperattenuating struts. While the metal skeleton is porous, it may be completely or partially covered with nonporous polyester graft material. The polyester graft material cannot be seen at CT, although a minority of stent-grafts have circumferential metallic rings that define the proximal and distal ends.

Some stent-graft systems include multiple pieces to accommodate the length of the aorta. Other stent-graft systems specifically designed for the aortic arch may contain fenestrae or built-in side branches to accommodate the arch vessels (18,19). Multiplanar reconstructions, maximum intensity projections (MIPs), and volumetric reconstructions are often of particular value in depicting endovascular stent-graft anatomy (20–22) (Fig 9).

Repair Techniques

The treatment approach to repair of the ascending aorta and aortic arch depends on patient

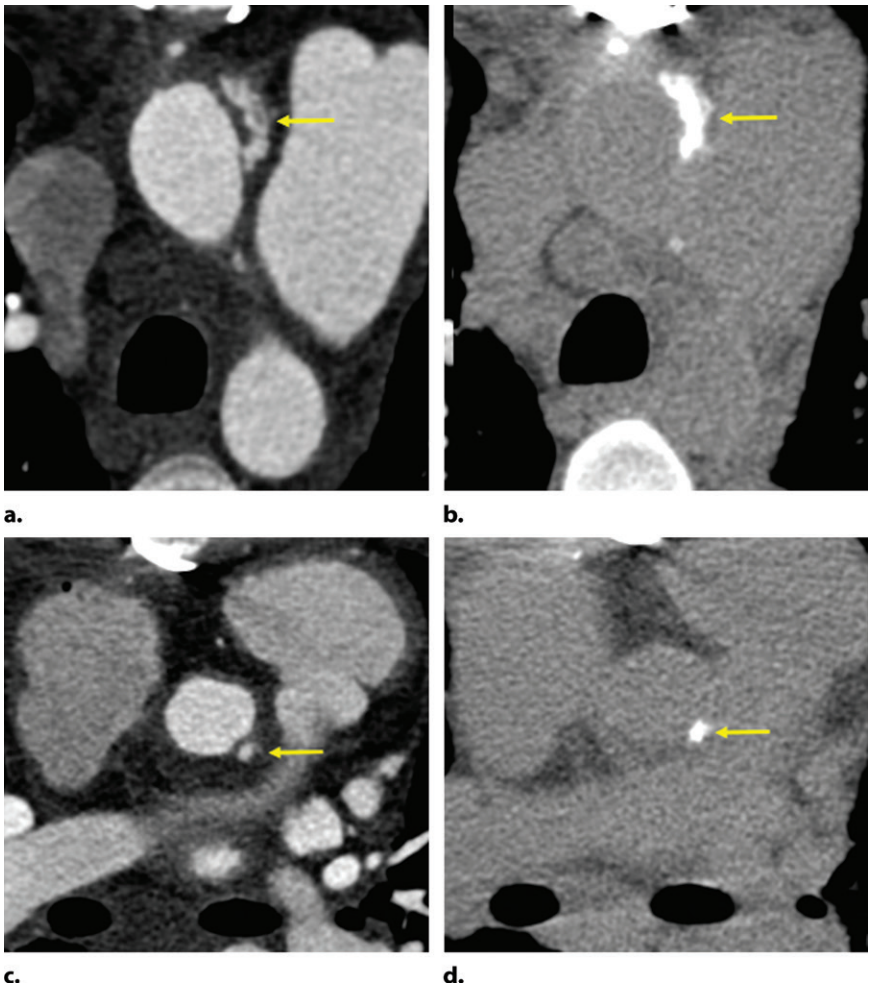

Figure 7. Felt pledgets in a 40-year-old woman after open surgical proximal aortic repair. **(a, b)** Axial contrast-enhanced **(a)** and noncontrast **(b)** CT images show a hyperattenuating structure (arrow) consistent with a felt pledget along the left anterolateral aspect of the aorta. **(c, d)** Axial contrast-enhanced **(c)** and noncontrast **(d)** CT images inferior to **a** and **b** show an additional pledget (arrow) along the left posterolateral aspect of the aorta. As shown here, felt pledgets can have different shapes. They are used liberally in open surgical repairs of the proximal aorta to control hemostasis, provide reinforcement, and seal off access sites. Awareness of felt pledgets prevents confusion with pseudoaneurysms. Although not typically required, noncontrast acquisitions can be used to confirm the presence of a hyperattenuating pledget.

characteristics, the specific pathologic condition encountered, and the anatomic extent of the needed repair. Repair of the ascending aorta alone is typically accomplished via open surgery. Repairs involving the aortic arch are more complicated because of the great vessels and may use combinations of surgical and endovascular techniques, often in staged procedures. To interpret postoperative studies after repair of the ascending aorta or aortic arch, the radiologist must understand the most common repair techniques and their expected imaging appearances. The following sections review these repairs, with specific attention directed to imaging features and the essential questions that distinguish the repairs to allow identification.

Zonal Anatomy

Aortic zones are used to describe the extent of the thoracic aorta that is repaired and the landing sites for endovascular stents when they are used. The Criado and Ishimaru classification systems for the thoracic aorta are similar and are shown in Figure 10 (23–25). In the Criado system, which is adopted by the Society for Vascular Surgery, zone 0 involves the ascending aorta and the origin of the innominate artery. Zone 1 spans the origin of the left common carotid artery, and zone 2 spans the origin of the left subclavian artery. Zone 3 extends from the distal aspect of the left subclavian artery through the first 2 cm of the descending aorta, with zone 4 extending distally.

Zone 3 of the Criado system presents a particular challenge for stent deployment, given that most endovascular stents require a 2-cm landing zone distal to the left subclavian artery to provide an adequate seal while avoiding coverage of the left subclavian artery during deployment. The Ishimaru system differs in that zone 3 extends from the distal aspect of the left subclavian artery to a border at the end of the curvature of the aortic arch (23,24,26).

Ascending Aorta (Zone 0)

Although new endovascular devices are being developed specifically for use in the ascending aorta, open surgery is currently used to manage almost all repairs of zone 0 (27–29). In describing a repair of the ascending aorta, the *first relevant question* is

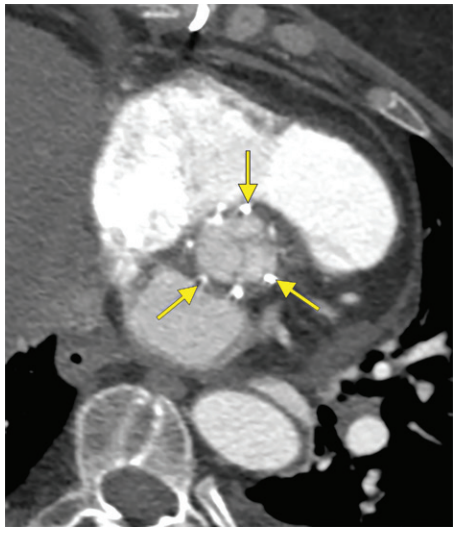

Figure 8. Automatic suture fasteners in a 65-year-old man after valve-sparing ascending aorta repair. Axial CT image shows metallic hyperattenuating structures (arrows) about the aortic annulus. These are Cor-Knot (LSI Solutions) automatic suture fasteners, which are used as a faster alternative to hand tying.

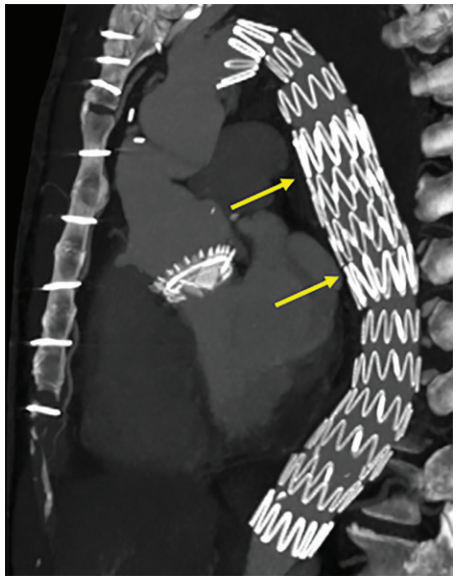

Figure 9. Endovascular stent-grafts in a 54-year-old man after combined proximal and descending aortic repair. Oblique sagittal MIP CT reconstruction shows the nitinol struts of the stent-grafts to advantage. In the mid descending aorta, a second stent with overlapping struts is present (arrows). This was placed to treat an endoleak.

whether the aortic valve has been repaired. Aortic valve repair can be achieved with a metallic or bioprosthetic valve, the former identifiable by hyperattenuating leaflets at CT and the latter having leaflets of native tissue attenuation but potentially accompanied by a ring scaffolding or suture anchors.

The *second relevant question* is whether the sinuses of Valsalva have been repaired. Patients who have undergone ascending aorta repair that begins distal to the sinuses of Valsalva have a supracoronary repair. Supracoronary repairs have the important advantage of not requiring reimplantation of the coronary arteries (30). Recognizing a supracoronary repair at CT requires identifying the anatomic configuration of the native sinuses of Valsalva and the coronary arteries, and that the repair begins at or above the sinotubular junction.

In a supracoronary repair, graft interfacing with the native aorta can be readily identified by the proximal felt ring, when present, as well as the redundant nonanatomic configuration. A distal felt ring in zone 0 may also be seen if repair of the arch was not performed. When a patient has combined surgery involving supracoronary repair and aortic valve replacement, this is known as the Wheat procedure (30,31) (Fig 11).

When an ascending aortic repair involves the sinuses of Valsalva, two major classes of techniques can be used: those that replace the native aortic valve and those that do not, otherwise known as valve-sparing surgeries. Surgeries that replace the aortic valve use a composite graft,

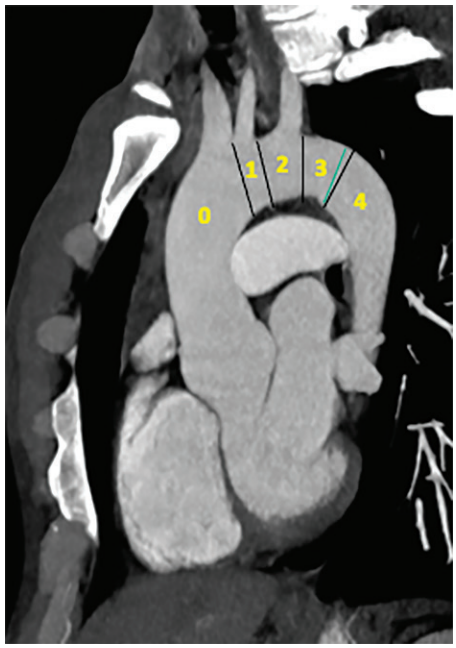

Figure 10. Oblique sagittal MIP CT image shows the aortic zones as defined by Criado et al (25).

which includes a mechanical or bioprosthetic valve fashioned into an ascending aortic graft. At CT, patients who have undergone composite graft aortic replacement have findings of a graft that begins at the valve plane and extends cranially. These grafts are typically tubular and may have folds or bends in them to accommodate their course in the mediastinum. When felt

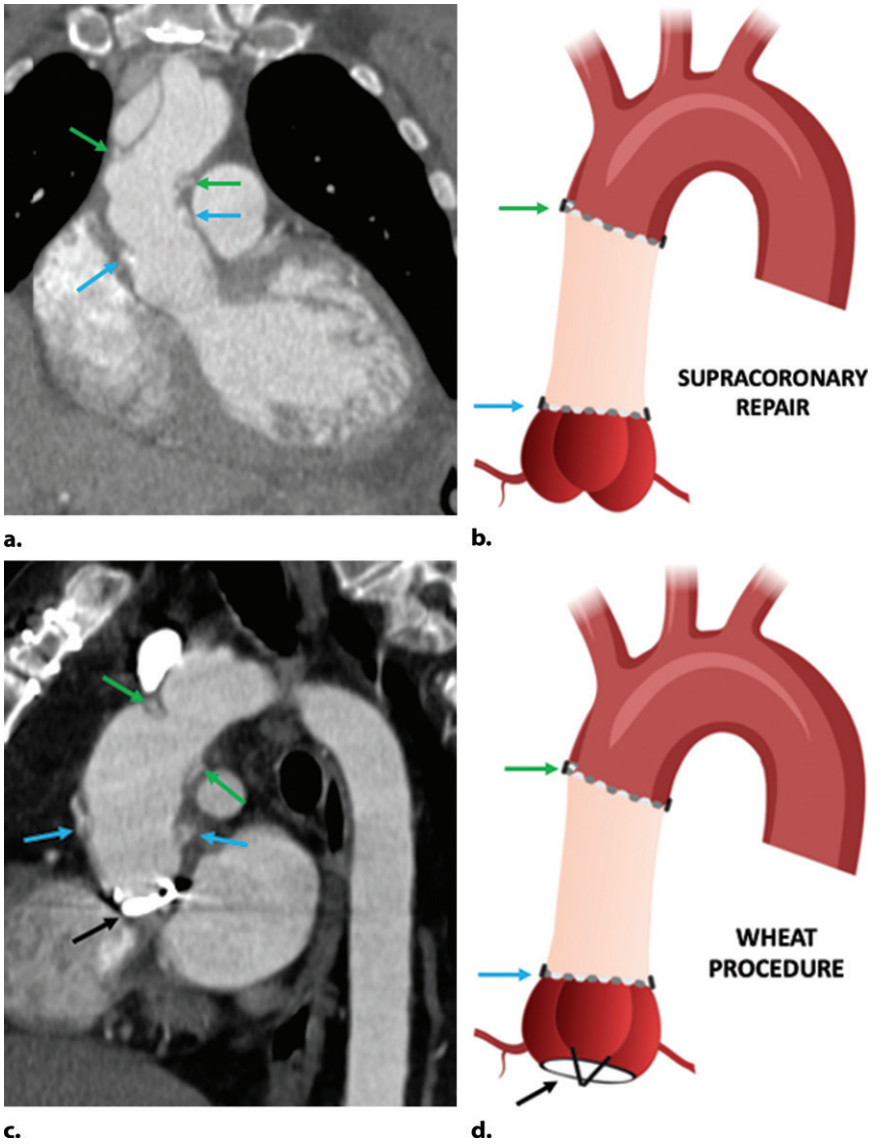

Figure 11. Supracoronary repairs. **(a)** Supracoronary repair in a 57-year-old man. Coronal CT image shows the repair, which is defined by felt rings at the sinotubular junction (blue arrows) and in the distal ascending aorta (green arrows). **(b)** Diagram of a supracoronary repair shows the proximal (blue arrow) and distal (green arrow) felt rings. **(c)** Supracoronary repair in a 62-year-old woman. Oblique sagittal CT image shows the repair, which is defined by felt rings at the sinotubular junction (blue arrows) and in the distal ascending aorta (green arrows). A mechanical aortic valve (black arrow) was placed at the same time, a combined surgery known as the Wheat procedure. **(d)** Diagram of the Wheat procedure shows the supracoronary repair, which is defined by proximal (blue arrow) and distal (green arrow) felt rings, as well as the mechanical aortic valve (black arrow). Supracoronary repairs are advantageous in that they do not require reimplantation of the coronary arteries.

rings are used, there will be only a distal felt ring, which allows distinction of a composite graft from a supracoronary graft. The normal anatomy of the sinuses of Valsalva will be absent, and the coronary arteries will be anastomosed (Fig 12).

Valve-sparing procedures were developed to allow repair of the ascending aorta below the level of the sinotubular junction while preserving the flow dynamics of the native aortic valve and avoiding the need for lifelong anticoagulation (32–36). The most common type of valve-sparing procedure is the David repair and its derivatives. In David-type repairs, the native aorta is excised and replaced with a graft in which the native aortic valve is resuspended. Of note, the aortic graft used in David repairs is typically sutured below the valve insertion, thus preventing further dilatation of the aortic root (37).

In David I repairs, the graft has a standard straight tubular configuration. In the T. David-V technique, a larger graft is used, which is cinched down at the annulus and neo–sinotubular junction (38). In the Demers-Miller or Stanford modification, two grafts are used, one smaller-caliber graft superiorly and a larger-caliber graft inferiorly. These modified techniques used to enlarge the graft at the root have the potential benefits of preserved flow dynamics and decreased contact of the leaflets with the graft, thus preserving valve durability (38).

At CT, David repairs will have only a distal felt ring, when present (39). In David I procedures, the graft will be relatively straight and tubular, while in the modified procedures it will have a subtle flare; in the two-graft Demers-Miller or Stanford modification, a reinforcing ring may be seen proximally at the neo–sinotubular junction. The sinuses of Valsalva are not individually reconstructed, and the coronary arteries will be reimplanted. The aortic valve will

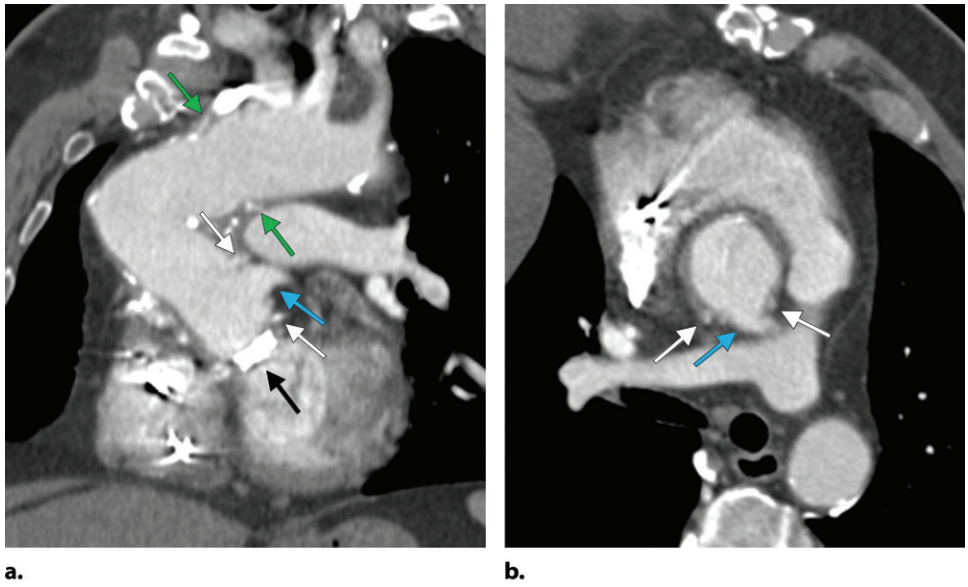

Figure 12. Composite graft repair of the ascending aorta with modified Bentall-type coronary artery anastomosis in a 49-year-old man. **(a)** Oblique coronal CT image shows the composite graft, which is defined by the mechanical aortic valve proximally (black arrow) and a felt ring distally (green arrows). The nonanatomic nature of the graft is evident, with its straight portions and associated acute angulation, lack of a normal waist at the sinotubular junction, and lack of normal sinuses of Valsalva. The coronary arteries were attached with a modified Bentall technique using a Carrel patch (blue arrow) and surrounding felt reinforcement (white arrows). **(b)** Oblique axial CT image at the level of the left main coronary artery anastomosis shows the Carrel patch (blue arrow) and surrounding felt reinforcement (white arrows). **(c)** Diagram of a composite graft of the ascending aorta shows a correlative distal felt ring (green arrow) and mechanical valve (black arrow). Also shown are diagrams of classic Bentall coronary anastomoses with tubular proximal portions versus flanged modified Bentall coronary anastomoses.

be native, although suture anchors may be seen proximally (Fig 13).

In the older but still occasionally encountered Yacoub repair, the native aorta is resected with the aortic valve left in place (32,40). The aorta is reconstructed with a scalloped graft that recreates neo–sinuses of Valsalva and attaches distal to the valve insertions and above the valve plane. At CT, the Yacoub repair has some of the same features as the valve-sparing David repair, including a native aortic valve, reimplanted coronary arteries, and a distal felt ring. The Yacoub repair can be distinguished on the basis of the characteristic appearance of the neo–sinuses of Valsalva and their distinct nonanatomic features, which are larger than would be expected and often have a sharp angulation at the neo–sinotubular junction (41–43) (Fig 14).

All surgeries that repair the sinuses of Valsalva require coronary reimplantation. How the coronary arteries were managed is the *third relevant question* for describing an ascending aortic repair. Understanding the expected imaging appearance of reimplanted coronary arteries is important, as it can aid in confirming that the sinuses of Valsalva have been repaired (when the extent of repair is unclear) and help prevent misidentification of the normal postoperative appearance as disease (42–44).

The Bentall technique is most commonly used and involves end-to-side anastomosis of the coronary artery to the aortic graft. In the classic Bentall technique, the coronary arteries are excised and directly reimplanted onto the graft. At CT, the proximal portions of coronary arteries repaired with the classic Bentall technique will be relatively cylindrical and may be only slightly larger at their origins.

In current practice, the classic Bentall technique has been modified, with a collar of normal

Figure 13. Valve-sparing David repairs. **(a)** David I repair of the ascending aorta in a 56-year-old man. Oblique coronal CT image shows a straight ascending aortic graft with a distal felt ring only (green arrows) and absence of the normal sinotubular junction and sinuses of Valsalva. The native aortic valve (yellow arrow) is present. The coronary artery anastomosis is also shown (white arrow). **(b)** Diagram of the David I repair shows its single felt ring (green arrow) and absence of normal anatomic features. **(c)** David-V Stanford modification repair in a 59-year-old woman. Oblique coronal CT image shows the distal felt ring (green arrow), distal graft (black arrow), and subtly larger proximal graft (blue arrows). **(d)** Diagrams of David repair modifications. Left: In the David V modification *(mod)*, a suture (orange arrow) is used to cinch the proximal graft. Green arrow = distal felt ring. Right: In the Demers-Miller/Stanford modification *(mod)*, two grafts are used: a smaller-caliber distal graft (black arrow) and a larger-caliber proximal graft (blue arrow). This results in a subtle caliber change between the grafts.

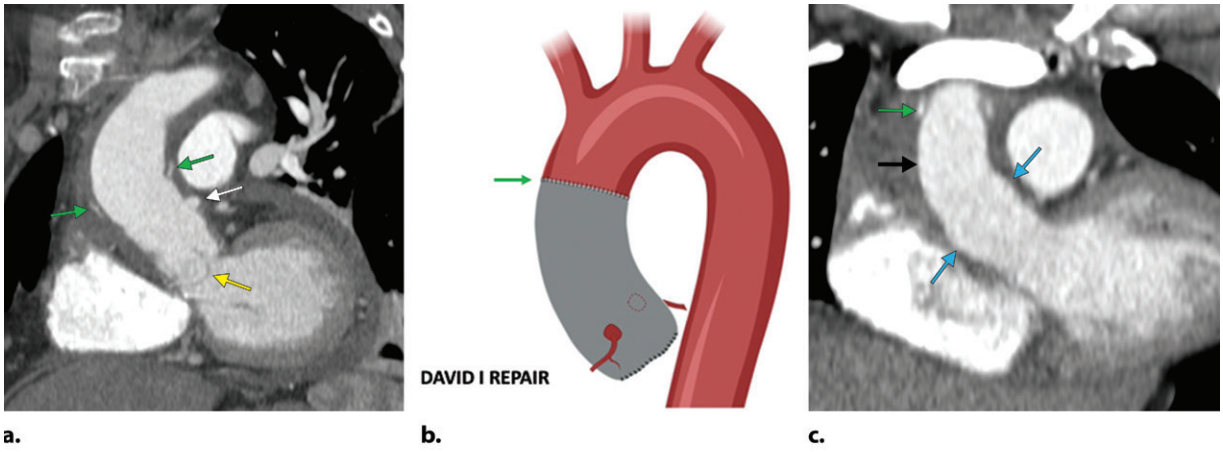

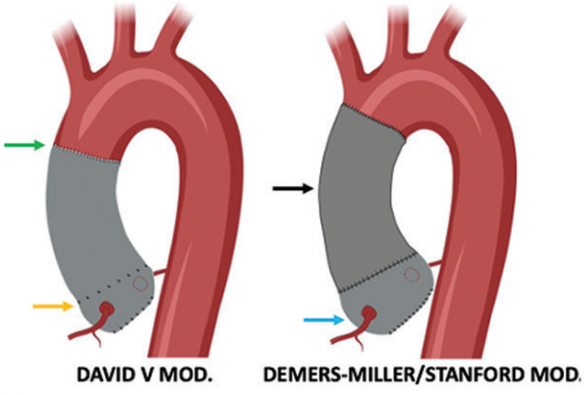

aorta excised around the coronary artery to fashion a flanged or trumpetlike configuration; this procedure, in which the proximal aspect of a vessel is harvested with a small portion of aorta, is known as a Carrel patch and reduces tension and kinking on the coronary anastomosis (41,45). The modified Bentall technique is preferred because it decreases operative time as well as overall morbidity and mortality, limiting complications such as excessive bleeding and subsequent development of unroofed coronary arteries or pseudoaneurysms.

When the coronary artery harvested with the modified Bentall technique is reimplanted on the aorta, postoperative CT will demonstrate the larger trumpetlike origin, which is typically reinforced with surrounding felt after it is sutured to produce what is termed a *coronary button* (46) (Fig 12). While there is no threshold size criterion for an abnormal modified Bentall coronary ostium, all reported cases of modified Bentall coronary artery pseudoaneurysms have exceeded 10 mm in diameter and enlarged over time (47,48).

In patients in whom the proximal coronary arteries or aorta are not suitable for creating an anastomosis, most often because of atherosclerotic disease or damage from a dissection, the Cabrol technique can be used, which allows utilization of more distal portions of the coronary arteries to create the anastomosis (49,50). In the Cabrol technique, a synthetic graft or transposed vessel is fashioned as a conduit and typically attached to the anterior aspect of the aorta (50). To extend to the left coronary arteries, the conduit most often has a retroaortic course, although it can have a course anterior to the aorta as well (51).

It is important to recognize a Cabrol conduit so that it is not mistaken for the false lumen of an aortic dissection (Fig 15). In certain circumstances, the Bentall and Cabrol techniques can both be used in the same patient for different coronary arteries. These can also be combined with traditional coronary artery bypass grafts if they are needed.

Frequently, composite grafts of the ascending aorta are generically referred to by the type of coronary anastomosis procedure performed. For example, patients who have received a composite graft with Bentall-type coronary artery anastomosis may be referred to as having undergone a "Bentall repair." We prefer to refer to these repairs as "composite grafting of the ascending aorta with a Bentall-type coronary anastomosis," thereby avoiding confusion with valve-sparing procedures that also use the Bentall and Cabrol

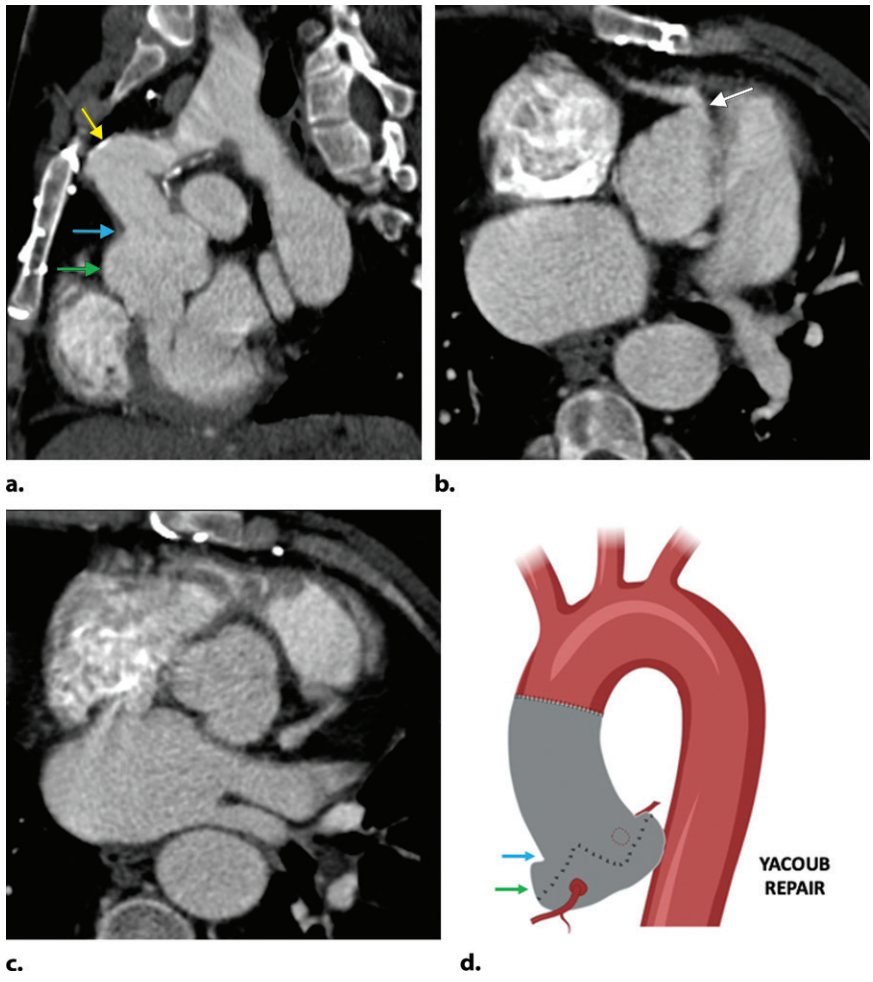

Figure 14. Valve-sparing Yacoub repair in a 28-year-old man. **(a)** Oblique sagittal CT image shows nonanatomic bulbous neo–sinuses of Valsalva (green arrow), a sharp near-90° angle at the neo–sinotubular junction (blue arrow), and a redundant graft of the tubular ascending aorta (yellow arrow), which has straight portions and an acute angle deviating to the left. **(b)** Axial CT image at the level of the right coronary anastomosis shows the Carrel patch morphology (arrow) used in the modified Bentall technique. **(c)** Oblique axial CT image inferior to **b** shows the bulbous reconstructed neo–sinuses of Valsalva. **(d)** Diagram of the Yacoub repair shows the scalloped graft (green arrow), which often produces bulbous neo–sinuses of Valsalva, with a sharp angle at the neo–sinotubular junction (blue arrow).

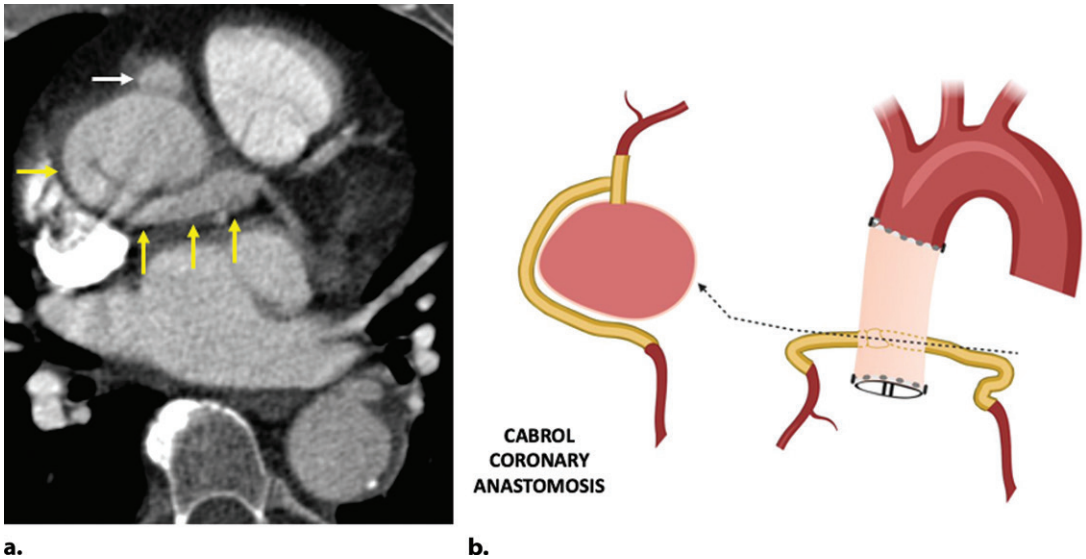

Figure 15. Cabrol coronary artery anastomosis in a 56-year-old man after composite aortic graft repair. **(a)** Oblique axial CT image shows the Cabrol coronary conduit for the left anterior descending and circumflex coronary arteries, which arises from the right anterior aspect of the aortic graft and takes a retroaortic course (yellow arrows). Understanding the expected appearance of a Cabrol conduit will prevent confusion with an intimomedial flap. This patient also has a separate Cabrol conduit for the right coronary artery (white arrow). **(b)** Diagram of a Cabrol coronary artery anastomosis shows the retroaortic course of the conduit (yellow) as it courses toward the left-sided coronary arteries.

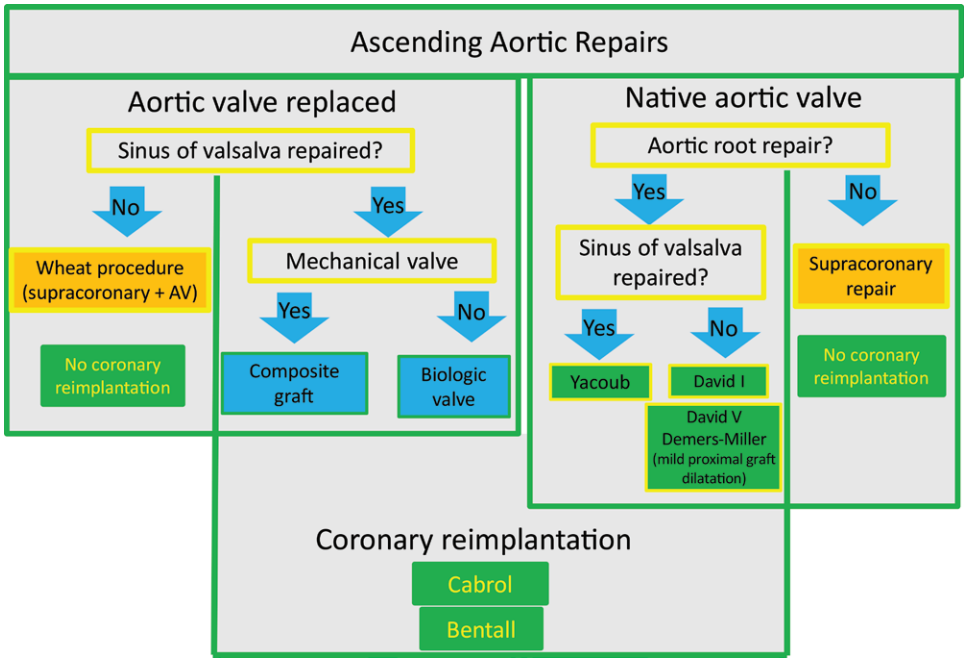

Figure 16. Chart summarizes ascending aortic repairs. *AV* = aortic valve.

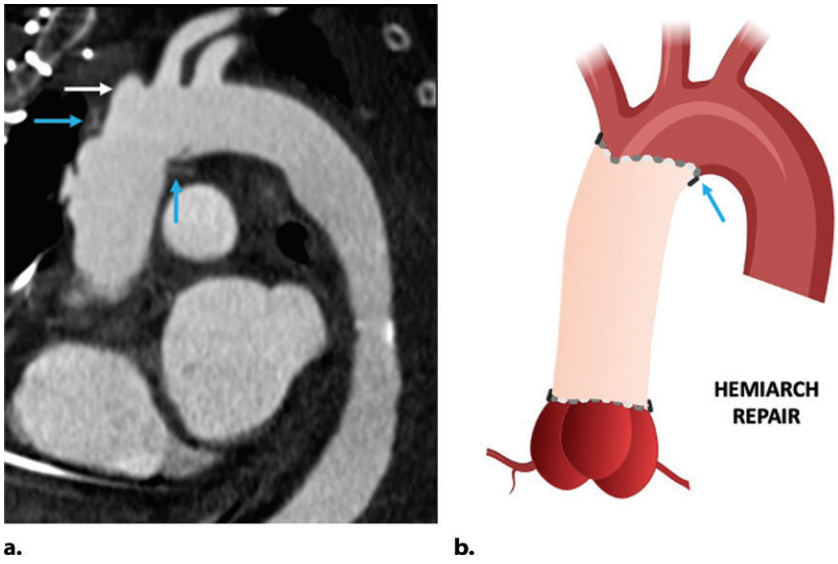

Figure 17. Hemiarch repair in a 48-year-old man. **(a)** Oblique sagittal CT reconstruction shows a felt ring (blue arrows), which denotes the distal extent of the graft along the lesser curvature of the aortic arch, opposite the innominate artery in zone 1 (white arrow). **(b)** Diagram shows a supracoronary-type hemiarch repair, with the beveled or tongue-shaped distal aspect of the graft (blue arrow) extending along the lesser curvature of the aortic arch.

coronary anastomosis procedures but do not involve replacing the aortic valve. A flowchart summarizing ascending aortic repairs is shown in Figure 16.

Aortic Arch and Beyond: Zones 1–4

Repairs involving the aortic arch are typically performed in conjunction with repairs of the ascending or descending aorta (13). It is important to note that the proximal extent of these repairs into zone 0 may be completed with any of the previously described techniques and can be extended to the level of the aortic valve. The simplest aortic arch repair involves extension of a zone 0 repair to the undersurface (or lesser curvature) of the aortic arch, a procedure often termed a *hemiarch repair* (52–55). The grafts used in hemiarch repairs have a distal portion that is tongue shaped (or beveled). At CT, the tongue-shaped extension can be shown to advantage on multiplanar reconstructions and will typically be reinforced with a combination of sutures and felt (Fig 17).

Repairs that involve the greater curvature of the aortic arch add an increased degree of complexity owing to necessary management of the arch vessels. While open surgical techniques are still used, hybrid and even entirely endovascular techniques are being increasingly employed in modern practice (18,26,27). Of note, arch repairs using an open surgical technique often

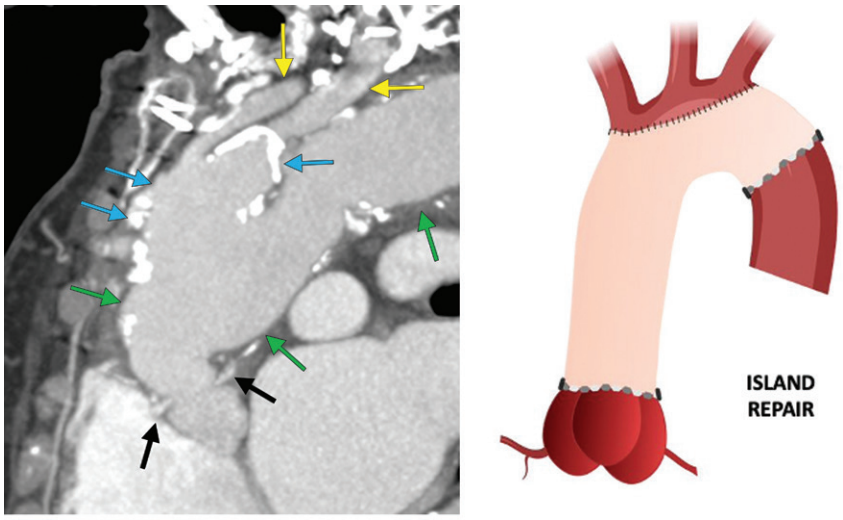

a. **b.**

Figure 18. Island patch repair technique of the great vessels in an 80-year-old woman with underlying chronic aortitis and ascending aortic and aortic arch elephant trunk–type repair. **(a)** Oblique sagittal CT reconstruction shows island repair (blue arrows) of the great vessels (yellow arrows); the island patch is attached to the cranial aspect of the open elephant trunk aortic graft (green arrows). Note that the island is dilated and heavily calcified, which may have been related to further wall inflammation after the original repair. A supracoronary felt ring (black arrows) is depicted proximally. **(b)** Diagram shows island repair management of the great vessels. Note that if the island does not dilate and there is no associated reinforcement material, it can be difficult to identify at CT. In this setting, identifying an island repair relies on recognizing that an open surgical graft has been used to repair the arch and that the arch vessels are native and without detectable anastomoses.

use a zone 2 repair approach, in which the arch is replaced to the level of zone 2 and the left subclavian artery is revascularized. Zone 2 repairs are beneficial, as they decrease the chance of injury to the left recurrent laryngeal nerve and improve surgical control of hemostasis (56).

To understand an arch repair at CT, the reader must determine how the arch vessels were managed. The "island patch" technique involves removing some or all of the aortic branch vessels and a portion of surrounding native aortic tissue en bloc and then reattaching them to an ovoid hole in a surgically placed open graft. At CT, the island patch technique can be recognized by identifying the piggyback nature of the island, a finding that may be accentuated in patients who have intrinsic abnormalities of the underlying aortic wall that result in continued dilatation of the island. Felt or sutures used to attach or reinforce the island may also be helpful, although they are often not present (46). In cases where the contour of the island is difficult to appreciate, a clue to an island repair is that the native arch vessels will retain their anatomic features and may contain atherosclerotic calcifications to the level of their origins; there will also be no caliber change to suggest an anastomosis to a tubular vascular graft (Fig 18).

In the debranching technique, the arch vessels are connected to longer tubular grafts, which are then attached to the ascending aorta or an ascending aorta graft. In many cases, particularly those with proximal attachment of the arch grafts, accompanying left carotid–left subclavian and carotid-carotid bypass may be used (13). At CT, patients who have undergone debranching procedures can be identified by recognizing the nonanatomic configuration of the branched grafts, which typically attach to the more proximal portion of the graft (57). Caliber changes and felt reinforcement material at the anastomoses of the arch vessel grafts with the native arch vessels are also frequently seen.

After debranching of the arch vessels, the tubular aortic arch can be managed with open or hybrid repair. Hybrid repairs of the aortic arch are classified into three types, which are described in Table 1 (58). Of note, type III hybrid procedures have the additional advantage of providing a geometrically advantageous landing zone for endovascular stent-grafts and can allow treatment of combined aortic arch and proximal descending aorta pathologic conditions without using an elephant trunk graft (Fig 19).

A third strategy for arch vessel management involves using a prefabricated graft that has separate extensions for each of the arch vessels. Using this type of prefabricated graft allows complete replacement of the native aortic arch. These grafts typically also contain a fourth side

Table 1: Types of Hybrid Aortic Arch Repairs with Important Imaging Findings

Type of Hybrid Aortic Arch Repair	Comments	Imaging Findings
I	Can be performed without cardiopulmonary bypass	Debranched arch vessels Endovascular stent in arch landing in zone 0 No open surgical graft
II	Can be performed in patients without suitable zone 0 landing site or who require concomitant zone 0 repair	Debranched arch vessels Zone 0 open surgical graft Endovascular stent in arch landing in the zone 0 open graft
III	Can be performed in patients with an inadequate landing site, who require extended repair of the aortic arch or descending aorta (open graft can be elephant trunk type) Provides improved geometry for endovascular stent deployment (more horizontal configuration of aortic arch)	Debranched arch vessels Open surgical graft extending from zone 0 to zone 1, 2, or 3—may be elephant trunk type Endovascular stent in arch landing in the open graft

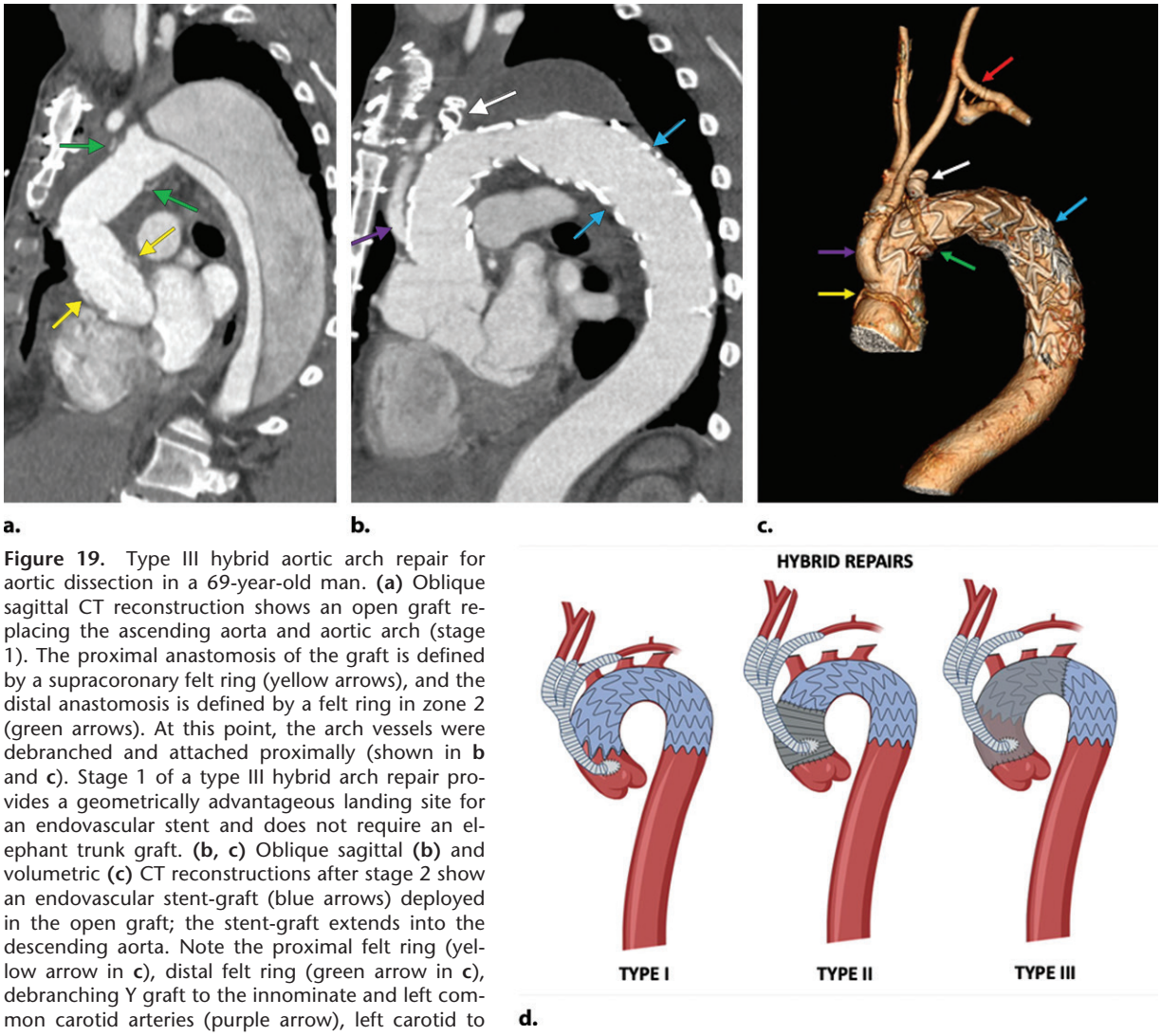

Figure 19. Type III hybrid aortic arch repair for aortic dissection in a 69-year-old man. **(a)** Oblique sagittal CT reconstruction shows an open graft replacing the ascending aorta and aortic arch (stage 1). The proximal anastomosis of the graft is defined by a supracoronary felt ring (yellow arrows), and the distal anastomosis is defined by a felt ring in zone 2 (green arrows). At this point, the arch vessels were debranched and attached proximally (shown in **b** and **c**). Stage 1 of a type III hybrid arch repair provides a geometrically advantageous landing site for an endovascular stent and does not require an elephant trunk graft. **(b, c)** Oblique sagittal **(b)** and volumetric **(c)** CT reconstructions after stage 2 show an endovascular stent-graft (blue arrows) deployed in the open graft; the stent-graft extends into the descending aorta. Note the proximal felt ring (yellow arrow in **c**), distal felt ring (green arrow in **c**), debranching Y graft to the innominate and left common carotid arteries (purple arrow), left carotid to subclavian bypass (red arrow in **c**), and left subclavian occluder (white arrow). **(d)** Diagram shows hybrid repairs of the aortic arch. See Table 1 for an explanation of the differences in these hybrid repairs.

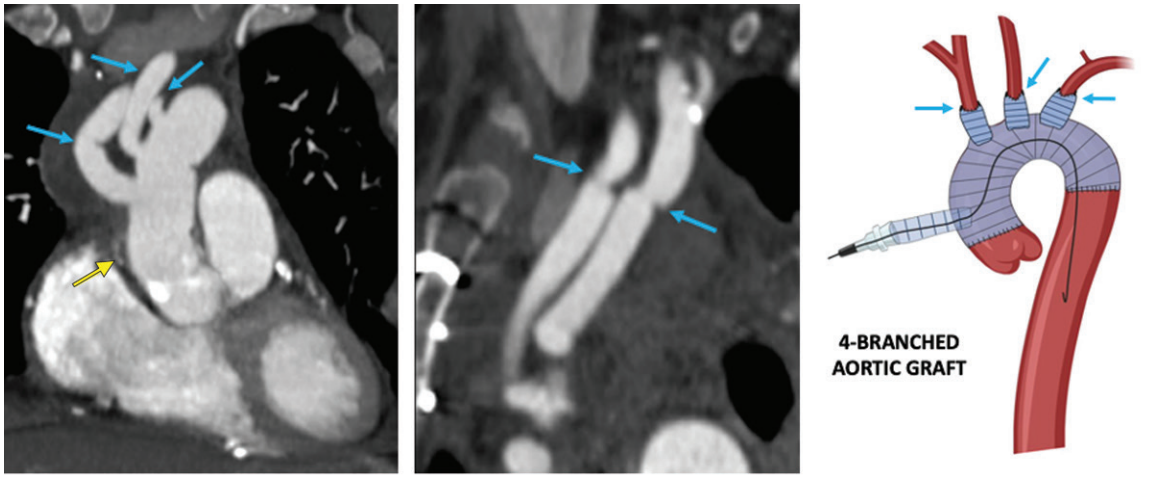

a. b. c.

Figure 20. Four-branched aortic arch graft in a 53-year-old man. **(a)** Oblique coronal CT reconstruction shows a branched ascending aortic and aortic arch graft with a felt ring proximally (yellow arrow), as well as individual graft branches for each of the great vessels (blue arrows). A fourth branch for bypass cannulation was also part of this graft, but was sealed with felt and is not shown at this obliquity. **(b)** Sagittal CT reconstruction along the course of the aortic arch grafts shows caliber changes (arrows) at the anastomoses of the graft branches with the innominate and left common carotid arteries. **(c)** Diagram shows a single-piece four-branched aortic arch graft. Note the caliber changes (arrows) at the anastomoses with the great vessels.

branch for cardiopulmonary bypass. At CT, these prefabricated grafts can be identified by recognizing anastomoses to the remaining portions of the arch vessels, which may have caliber changes and reinforcement material. In addition, the cannulation side branch will typically be occluded by a surgical clip or a combination of pledgets and sutures. The margins of a branched graft will typically be reinforced with a felt ring at its interface with the normal aorta (13,59,60) (Fig 20).

Improvements in endovascular techniques, as well as development of endovascular stent-grafts suited for the aortic arch, now allow novel repairs that do not necessarily require open surgery (61–63). These procedures can be recognized at imaging by the presence of combinations of endovascular stent-grafts rather than open grafts (24). In endovascular repairs, the arch vessels may be managed using the chimney or snorkel technique, in which stent-grafts are deployed in the arch vessels that then run alongside an endovascular graft deployed in the aortic arch (Fig 21) (64–66). Some endovascular stent-grafts specifically designed for the aortic arch have fenestrae or uncovered portions that communicate with the arch vessels or allow deployment of stents from the arch vessels into the lumen of the endovascular graft (18,67) (Fig 22). Other newer arch stent-grafts have branched or multipart configurations and may not require use of separate grafts for the arch vessels (61,62).

Some repairs terminate in the aortic arch, but more commonly they are extended into zones 3 and 4. This presents an important surgical issue in the setting of an open graft, as exposure of zones 3 and 4 typically requires a lateral thoracotomy and hence a separate surgical procedure. Open surgical aortic arch grafts are most commonly extended distally using the elephant trunk technique, which was originally a two-stage procedure (68). Stage I involves a median sternotomy with open repair of all or part of the arch or ascending aorta using an elephant trunk graft. At CT, patients who have undergone only stage I of an elephant trunk repair will have an open graft of the aortic arch or ascending aorta, typically demarcated by felt rings proximally and also distally at the level of the graft extending into the lumen of the unrepaired more distal aorta (69). The arch vessels will have findings of management with debranching, a branched graft, or the island patch technique. Most notably, the elephant trunk graft will be identifiable at imaging, extending into the lumen of the descending aorta as two parallel hypoattenuating linear structures that may have metallic clips at their tips (69).

It is important to recognize the appearance of elephant trunk grafts in patients who have undergone only stage I repairs, as the dangling elephant trunk can be mistaken for an intimomedial flap. Differentiation can be achieved by identifying the parallel nature of the walls of the graft as well as the proximal extent of the graft, which will typically be defined by reinforcement material or a subtle caliber change.

In a traditional elephant trunk repair, after a recovery period, the patient returns for open repair of the descending aorta, in which a lateral thoracotomy is performed to replace the descending

Figure 21. Endovascular repair of aortic zones 0–4 using the chimney technique in a 55-year-old man. **(a)** Oblique sagittal MIP CT reconstruction shows a stent-graft in the ascending aorta and aortic arch (yellow arrows) (landing in zone 0), with additional stent-grafts in the innominate and left common carotid arteries (blue arrows). The great-vessel stents are tunneled next to the aortic graft using the chimney technique. The left subclavian artery is occluded proximally and revascularized (not shown). **(b)** CT reconstruction perpendicular to the proximal portion of the aortic graft shows that the stent-grafts deployed in the innominate and left common carotid arteries (blue arrow) travel outside the stent in the aorta (yellow arrows). **(c)** Diagram shows endovascular aortic arch repair using the chimney technique.

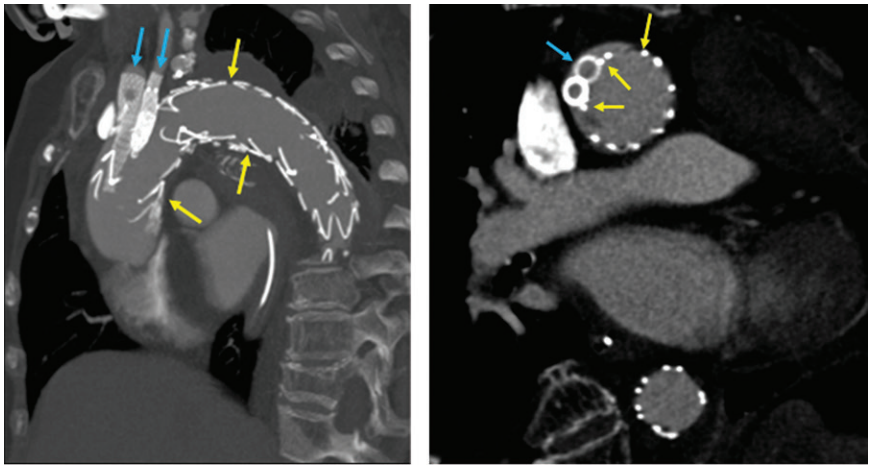

a. **b.**

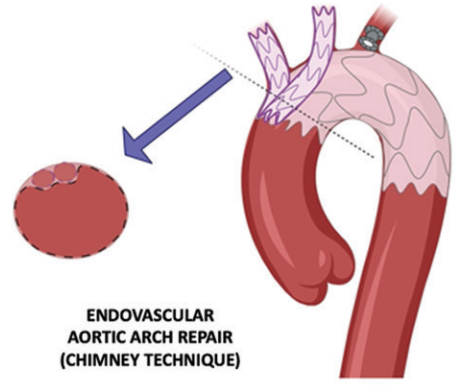

c.

aorta with a second open graft, which is anastomosed to the distal aspect of the elephant graft, resulting in a contiguous repair with graft-to-graft anastomoses along the course of the ascending aorta, aortic arch, and descending aorta (68). While traditional elephant trunk repairs requiring two open surgeries are still occasionally performed, they have largely been replaced by hybrid procedures, in which the second stage of the elephant trunk repair is achieved via deployment of an endovascular stent inside the elephant trunk graft; this can be performed at the time of the initial procedure or after a period of recovery. The endovascular stent can be placed in a retrograde fashion via femoral cannulation or antegrade through the open graft, aorta, or axillary artery.

These newer antegrade placements of the stent-graft have several names. The frozen elephant trunk procedure involves antegrade placement of the stent-graft, which is then anchored (or "frozen") at its distal deployment site. In the buffalo trunk procedure, a modified composite graft incorporating a soft portion for the arch and an endovascular stent-graft for the descending aorta is prepared and deployed as a unit (56,58,70–72). Another variation, the reverse elephant trunk, involves treatment of the descending aorta first via placement of an endovascular stent through the transected aorta, followed by construction of the surgical graft to the stent (13).

In all elephant trunk variations, the CT appearance will be similar, with *(a)* findings of open surgical repair of the proximal aorta with managed arch vessels (island, debranching, or four-branched surgical graft) and *(b)* an endovascular stent extending into the distal aspect of the open graft. In addition to a felt ring at the proximal margin of the open surgical graft, a distal felt ring may be used to reinforce the anastomosis between the graft and the native distal aorta, with the elephant trunk portion extending beyond it (3,58) (Fig 23).

Complications

Some of the most feared complications of ascending aorta and aortic arch repair, including stroke and paralysis, do not have associated thoracic CT findings (52,53). However, imaging does play an important role in investigation of many postoperative complications and is also used in routine follow-up of these patients. Complications can largely be divided into findings consistent with

Figure 22. Endovascular repair of aortic zones 0–4 using a fenestrated endovascular stent-graft in a 53-year-old man. **(a)** Oblique sagittal MIP CT reconstruction shows a fenestrated scalloped graft (yellow arrows) deployed in the aorta and landing in zone 0. The fenestrae (green arrows) can be identified along its greater curvature. Individual stents from the brachiocephalic and left common carotid arteries (blue arrows) were tunneled into the aortic graft via direct open cannulation of their respective arteries. An occluder device (red arrow) is depicted in the proximal left subclavian artery. Owing to an endoleak, a second stent was deployed in the mid descending aorta during a subsequent procedure (white arrow). **(b)** CT reconstruction perpendicular to the proximal aspect of the aortic stent-graft shows the great-vessel stents (blue arrows) within the fenestrated aortic stent (yellow arrows), allowing differentiation from a chimney-type repair, as shown in Figure 21. **(c)** Diagram shows endovascular aortic arch repair using a fenestrated graft.

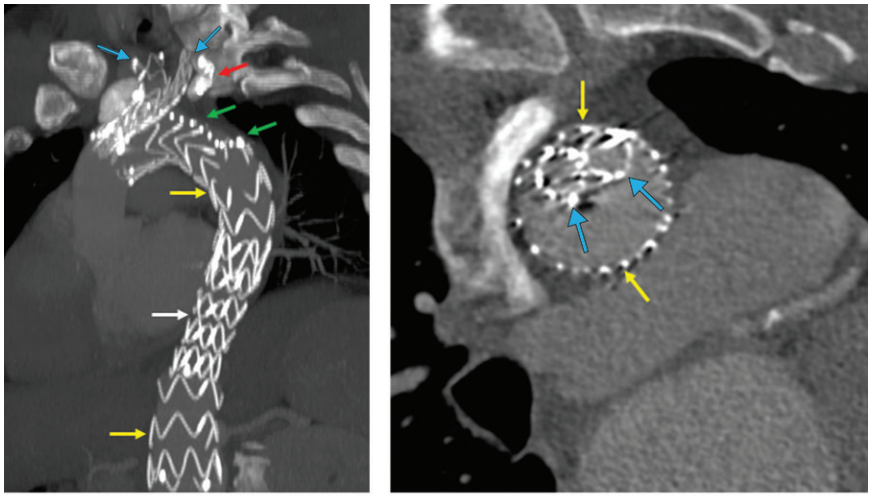

a. b.

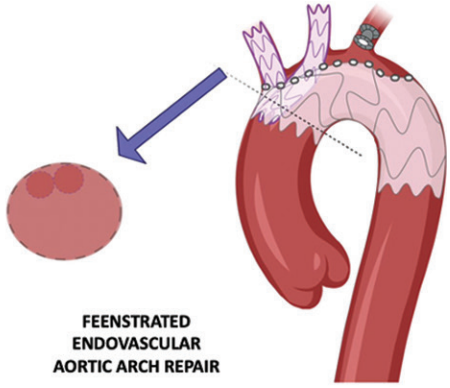

c.

breakdown or infection of the repair, complications affecting the adjacent remaining native aorta, and complications specific to endografts, when present. Recognizing complications at CT primarily relies on identifying deviations from the expected postoperative appearance. In addition to understanding the repair itself, the radiologist must also be aware of expected findings in the surrounding soft tissues, particularly in assessing for infection and hemorrhage in the recent postoperative period.

Patients who have undergone ascending aorta and aortic arch repairs, particularly via open surgery, will have fluid and hematoma in the mediastinum weeks after surgery, which may be related to the repair itself or the treated pathologic condition (42,44). Over time, the fluid and hematoma evolve, typically becoming lower in attenuation. Gas bubbles—which may be initially present—should also resolve. As these fluid collections resolve, they may even develop mild peripheral thickening or enhancement. In some situations, they may recur, particularly when drains are removed (Fig E1).

Indeed, Sundaram et al (43) evaluated 20 patients with postoperative "perigraft low-attenuation material" detected at CT and found that only eight were proved to have infection. As such, fluid in the mediastinum as well as other complications of repairs, including pseudoaneurysms, must be considered in the context of the patient's clinical presentation and correlated with fever, elevated white blood cell (WBC) count, and results of blood cultures.

In many cases, definitive evaluation is a two-step process that begins with identifying concerning imaging findings, which are then investigated with surgical exploration or percutaneous sampling. In difficult cases where surgical exploration is considered high risk or there have been negative aspirates of fluid, consideration can be given to fluorodeoxyglucose (FDG) PET/CT or indium 111 WBC scanning to support or refute the presence of an active infection. Important complications, support-

Figure 23. Elephant trunk repairs. **(a)** Stage I of an elephant trunk repair for aortic dissection in a 63-year-old man. Oblique axial CT reconstruction centered in the proximal descending aorta shows the relatively parallel walls of the elephant trunk graft (white arrows) extending into the aneurysmal descending thoracic aorta (yellow arrows). Redundancy at the level of the proximal descending aorta at the distal graft attachment site (blue arrows) is due to inverted oversewing performed as part of the modified elephant trunk surgical technique. **(b)** Reverse elephant trunk repair in a 64-year-old woman. The repair first involved antegrade placement of an endovascular stent into the transected proximal descending aorta, followed by debranching of the great vessels and construction of an open surgical ascending aortic and aortic arch graft to the already deployed stent; this was accomplished in a single surgical procedure. Oblique sagittal CT reconstruction shows an endovascular stent (white arrows) in the descending aorta (yellow arrows) and an ascending aortic supracoronary and arch graft (blue arrows) with a proximal felt ring (green arrow) and a nonanatomic configuration, with straight portions and acute angulation. A felt ring (orange arrow) is also depicted at the junction of the open and endovascular grafts. **(c)** Diagram shows elephant trunk repairs. The hybrid elephant trunk repair can be accomplished in one procedure, in which open surgical repair of the ascending aorta and aortic arch as well as endovascular stent placement in the more distal aorta are both performed.

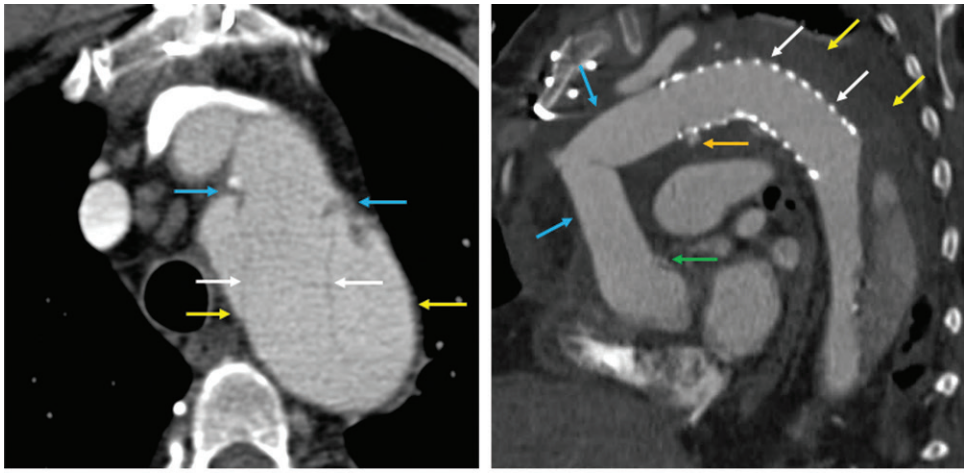

a. b.

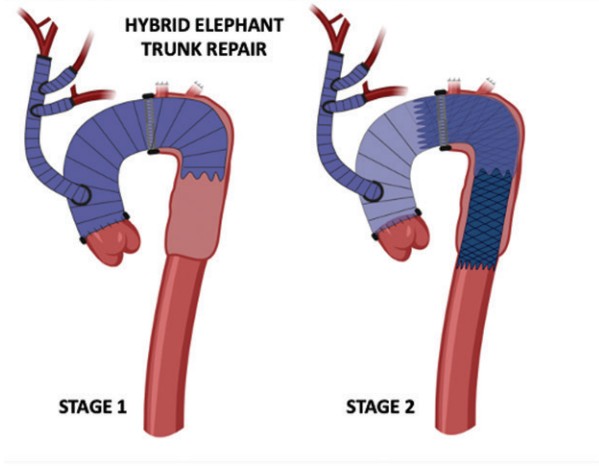

c.

ive CT findings, and potential mimics are summarized in Table 2, with representative examples in Figures E2–E7 (20,42–44).

Conclusion

Patients who have undergone repair of the ascending aorta and aortic arch represent an important challenge for the diagnostic radiologist. Recognition of the commonly used repair components is the first step in interpreting CT studies in these patients. The second step requires knowledge of the commonly employed repair techniques and their expected CT appearances. This is facilitated by a structured approach to the imaging findings focusing on the key questions that define the differences between repairs.

Given the use of new and combined techniques, radiologists will frequently need to go beyond basic knowledge and use operative notes for complete understanding of complicated cases. Deviations from the expected imaging appearance are key to identifying postoperative complications. By using this practical approach, radiologists will produce relevant interpretations and facilitate improved communication with surgeons and other referring clinicians.

Acknowledgments.—Stylized aortic diagrams were created using BioRender software *(https://biorender.com/)*.

References

1. Kouchoukos NT, Karp RB, Blackstone EH, Kirklin JW, Pacifico AD, Zorn GL. Replacement of the ascending aorta and aortic valve with a composite graft: results in 86 patients. Ann Surg 1980;192(3):403–413.
2. Prescott-Focht JA, Martinez-Jimenez S, Hurwitz LM, et al. Ascending thoracic aorta: postoperative imaging evaluation. RadioGraphics 2013;33(1):73–85.
3. Hoang JK, Martinez S, Hurwitz LM. MDCT angiography of thoracic aorta endovascular stent-grafts: pearls and pitfalls. AJR Am J Roentgenol 2009;192(2):515–524.

Table 2: Types of Potential Complications of Ascending Aorta and Aortic Arch Repairs, Supportive CT Findings, and Potential Mimics

Complication Type*	Supportive CT Findings	Potential Mimics
Infection (Figs E2, E3)	Fluid collection Persistent gas bubbles Inflammatory fat stranding Sternal dehiscence or osteomyelitis Infectious pseudoaneurysm Irregular border, may be saccular with a narrow neck, associated with inflammatory stranding, grows rapidly, extravasation if ruptured Valve thickening or endocarditis Distal infectious emboli Fistula	Seroma Hematoma Lymphocele Infarcting omental flap Sternal resorption for healing Noninfected pseudoaneurysm Reinforcement material Side grafts
Noninfected breakdown (Fig E4)	Noninfected pseudoaneurysm Paucity of inflammatory stranding, may be slow growing in chronic phase if contained by adhesions or inclusion graft, located at sites of potential breakdown including anastomoses and cannulation sites Displaced reinforcement material at access or cannulation site	Infectious pseudoaneurysm Reinforcement material Side grafts Carrel patch
Hemorrhage (Fig E5)	High-attenuating (>30 HU) collection adjacent to graft or access site with possible extravasation	Postoperative blood Infarcting omental fat Reinforcement material Calcium
Endograft or hybrid repair (Fig E6)	Endoleaks Types I and III have increased incidence in thoracic endografts versus abdominal endografts; type II from left subclavian artery can fill in arterial phase and contribute considerable flow to excluded aorta In hybrid repairs, dehiscence of open elephant graft component Stent migration False lumen deployment Stent collapse	Stent beaking in arch Calcium Reinforcement material
Adjacent aorta (Fig E7)	Aneurysm Dissection or intramural hematoma Initial postsurgery imaging: may be iatrogenic Dissections below supracoronary graft at root may be managed conservatively if stable	Yacoub reconstruction Graft folds Stage I elephant trunk repair Cabrol conduit

*Numbers in parentheses are example figures.

4. Dossche KM, de la Rivière AB, Morshuis WJ, Schepens MAAM, Defauw JJAM, Ernst SM. Cryopreserved aortic allografts for aortic root reconstruction: a single institution's experience. Ann Thorac Surg 1999;67(6):1617–1622.
5. Preventza O, Mohamed AS, Cooley DA, et al. Homograft use in reoperative aortic root and proximal aortic surgery for endocarditis: a 12-year experience in high-risk patients. J Thorac Cardiovasc Surg 2014;148(3):989–994.
6. Kouchoukos NT, Masetti P, Nickerson NJ, Castner CF, Shannon WD, Dávila-Román VG. The Ross procedure: long-term clinical and echocardiographic follow-up. Ann Thorac Surg 2004;78(3):773–781; discussion 773–781.
7. Lim E, Ali A, Theodorou P, et al. Longitudinal study of the profile and predictors of left ventricular mass regression after stentless aortic valve replacement. Ann Thorac Surg 2008;85(6):2026–2029.
8. Hanneman K, Chan FP, Mitchell RS, Miller DC, Fleischmann D. Pre- and Postoperative Imaging of the Aortic Root. RadioGraphics 2016;36(1):19–37.
9. Bentall H, De Bono A. A technique for complete replacement of the ascending aorta. Thorax 1968;23(4):338–339.
10. Niederhäuser U, Rüdiger H, Künzli A, et al. Surgery for acute type A aortic dissection: comparison of techniques. Eur J Cardiothorac Surg 2000;18(3):307–312.
11. Quint LE, Francis IR, Williams DM, Monaghan HM, Deeb GM. Synthetic interposition grafts of the thoracic aorta: postoperative appearance on serial CT studies. Radiology 1999;211(2):317–324.
12. Sundaram B, Quint LE, Patel HJ, Deeb GM. CT findings following thoracic aortic surgery. RadioGraphics 2007;27(6):1583–1594.
13. Zanotti G, Reece TB, Aftab M. Aortic Arch Pathology: Surgical Options for the Aortic Arch Replacement. Cardiol Clin 2017;35(3):367–385.
14. Riesenman PJ, Farber MA, Mendes RR, Marston WA, Fulton JJ, Keagy BA. Coverage of the left subclavian artery during thoracic endovascular aortic repair. J Vasc Surg 2007;45(1):90–94; discussion 94–95.

15. Caronno R, Piffaretti G, Tozzi M, Lomazzi C, Rivolta N, Castelli P. Intentional coverage of the left subclavian artery during endovascular stent graft repair for thoracic aortic disease. Surg Endosc 2006;20(6):915–918.
16. Tiesenhausen K, Hausegger KA, Oberwalder P, et al. Left subclavian artery management in endovascular repair of thoracic aortic aneurysms and aortic dissections. J Card Surg 2003;18(5):429–435.
17. El-Sherief AH, Wu CC, Schoenhagen P, et al. Basics of cardiopulmonary bypass: normal and abnormal postoperative CT appearances. RadioGraphics 2013;33(1):63–72.
18. Tsilimparis N, Debus ES, von Kodolitsch Y, et al. Branched versus fenestrated endografts for endovascular repair of aortic arch lesions. J Vasc Surg 2016;64(3):592–599.
19. Tsilimparis N, Drewitz S, Detter C, et al. Endovascular Repair of Ascending Aortic Pathologies With Tubular Endografts: A Single-Center Experience. J Endovasc Ther 2019;26(4):439–445.
20. Hoang JK, Martinez S, Hurwitz LM. MDCT angiography after open thoracic aortic surgery: pearls and pitfalls. AJR Am J Roentgenol 2009;192(1):W20–W27.
21. Batra P, Bigoni B, Manning J, et al. Pitfalls in the diagnosis of thoracic aortic dissection at CT angiography. RadioGraphics 2000;20(2):309–320.
22. Riley P, Rooney S, Bonser R, Guest P. Imaging the postoperative thoracic aorta: normal anatomy and pitfalls. Br J Radiol 2001;74(888):1150–1158.
23. Upchurch GR Jr, Escobar GA, Azizzadeh A, et al. Society for Vascular Surgery clinical practice guidelines of thoracic endovascular aortic repair for descending thoracic aortic aneurysms. J Vasc Surg 2021;73(1S):55S–83S.
24. Mitchell RS, Ishimaru S, Ehrlich MP, et al. First International Summit on Thoracic Aortic Endografting: roundtable on thoracic aortic dissection as an indication for endografting. J Endovasc Ther 2002;9(suppl 2):II98–II105.
25. Criado FJ, Clark NS, Barnatan MF. Stent graft repair in the aortic arch and descending thoracic aorta: a 4-year experience. J Vasc Surg 2002;36(6):1121–1128.
26. Ishimaru S. Endografting of the aortic arch. J Endovasc Ther 2004;11(suppl 2):II62–II71.
27. Ahmed Y, Houben IB, Figueroa CA, et al. Endovascular ascending aortic repair in type A dissection: a systematic review. J Card Surg 2021;36(1):268–279.
28. Uchida K, Minami T, Cho T, et al. Results of ascending aortic and arch replacement for type A aortic dissection. J Thorac Cardiovasc Surg doi: 10.1016/j.jtcvs.2020.02.087. Published online March 7, 2020. Accessed December 8, 2020.
29. Ghoreishi M, Shah A, Jeudy J, et al. Endovascular Repair of Ascending Aortic Disease in High-Risk Patients Yields Favorable Outcome. Ann Thorac Surg 2020; 109(3):678–685.
30. Wheat MW Jr, Wilson JR, Bartley TD. Successful replacement of the entire ascending aorta and aortic valve. JAMA 1964;188(8):717–719.
31. Yoda M, Nonoyama M, Shimakura T, Morishita A, Takasaki T. Surgical Case of Aortic Root and Thoracic Aortic Aneurysm after the Wheat Procedure. Ann Thorac Cardiovasc Surg 2002;8(2):115–118.
32. Harky A, Antoniou A, Howard C, Rimmer L, Ahmad MU, Bashir M. Valve sparing aortic root surgery: from revolution to evolution? J Vis Surg 2019;5:14.
33. Tian D, Rahnavardi M, Yan TD. Aortic valve sparing operations in aortic root aneurysms: remodeling or reimplantation? Ann Cardiothorac Surg 2013;2(1):44–52.
34. Charitos EI, Sievers HH. Anatomy of the aortic root: implications for valve-sparing surgery. Ann Cardiothorac Surg 2013;2(1):53–56.
35. David TE, Armstrong S, Ivanov J, Feindel CM, Omran A, Webb G. Results of aortic valve-sparing operations. J Thorac Cardiovasc Surg 2001;122(1):39–46.
36. David TE, Ivanov J, Armstrong S, Feindel CM, Webb GD. Aortic valve-sparing operations in patients with aneurysms of the aortic root or ascending aorta. Ann Thorac Surg 2002;74(5):S1758–S1761; discussion S1792–S1799.
37. Miller DC. Valve-sparing aortic root replacement in patients with the Marfan syndrome. J Thorac Cardiovasc Surg 2003;125(4):773–778.
38. Demers P, Miller DC. Simple modification of "T. David-V" valve-sparing aortic root replacement to create graft pseudosinuses. Ann Thorac Surg 2004;78(4):1479–1481.
39. Fleischmann D, Liang DH, Mitchell RS, Miller DC. Pre- and postoperative imaging of the aortic root for valve-sparing aortic root repair (V-SARR). Semin Thorac Cardiovasc Surg 2008;20(4):365–373.
40. Bechtel JFM, Erasmi AW, Misfeld M, Sievers HH. Reconstructive surgery of the aortic valve: the Ross, David, and Yacoub procedures [in German]. Herz 2006;31(5):413–422.
41. Cherry C, DeBord S, Hickey C. The modified Bentall procedure for aortic root replacement. AORN J 2006;84(1):52–55, 58–70; quiz 71–74.
42. Chu LC, Johnson PT, Cameron DE, Fishman EK. MDCT evaluation of aortic root surgical complications. AJR Am J Roentgenol 2013;201(4):736–744.
43. Sundaram B, Quint LE, Patel S, Patel HJ, Deeb GM. CT appearance of thoracic aortic graft complications. AJR Am J Roentgenol 2007;188(5):1273–1277.
44. Green DB, Vargas D, Reece TB, Raptis CA, Johnson WR, Truong QA. Mimics of Complications in the Postsurgical Aorta at CT. Radiol Cardiothorac Imaging 2019;1(4):e190080.
45. Milano AD, Pratali S, Mecozzi G, et al. Fate of coronary ostial anastomoses after the modified Bentall procedure. Ann Thorac Surg 2003;75(6):1797–1801; discussion 1802.
46. Bang TJ, Green DB, Reece TB, DaBreo D, Vargas D. Contemporary Imaging Findings in Aortic Arch Surgery. Curr Radiol Rep 2019;7(12):32.
47. Dagenais F, Cartier R, Paquet E, Hudon G, Castonguay Y, Leclerc Y. Pseudoaneurysm after Bentall repair: magnetic resonance imaging assessment. Can J Cardiol 1993;9(10):869–872.
48. Okamoto K, Casselman FP, De Geest R, Vanermen H. Giant left coronary ostial aneurysm after modified Bentall procedure in a Marfan patient. Interact Cardiovasc Thorac Surg 2008;7(6):1164–1166.
49. Cabrol C, Pavie A, Gandjbakhch I, et al. Complete replacement of the ascending aorta with reimplantation of the coronary arteries: new surgical approach. J Thorac Cardiovasc Surg 1981;81(2):309–315.
50. Gelsomino S, Frassani R, Da Col P, et al. A long-term experience with the Cabrol root replacement technique for the management of ascending aortic aneurysms and dissections. Ann Thorac Surg 2003;75(1):126–131.
51. Kruser TJ, Osaki S, Kohmoto T, Chopra PS. Computed tomography finding mimicking aortic dissection after Cabrol procedure. Asian Cardiovasc Thorac Ann 2009;17(1):108–109.
52. Kreibich M, Rylski B, Czerny M, et al. Influence of Age and the Burden of Ischemic Injury on the Outcome of Type A Aortic Dissection Repair. Ann Thorac Surg 2019;108(5):1391–1397.
53. Merkle J, Sabashnikov A, Deppe AC, et al. Impact of ascending aortic, hemiarch and arch repair on early and long-term outcomes in patients with Stanford A acute aortic dissection. Ther Adv Cardiovasc Dis 2018;12(12):327–340.
54. Sultan I, McGarvey J, Vallabhajosyula P, Desai ND, Bavaria JE, Szeto WY. Routine use of hemiarch during acute type A aortic dissection repair. Ann Cardiothorac Surg 2016;5(3):245–247.
55. Itoh A, Fischbein M, Arata K, Miller DC. "Peninsula-style" transverse aortic arch replacement in patients with bicuspid aortic valve. Ann Thorac Surg 2010;90(4):1369–1371.
56. Eldeiry M, Aftab M, Bergeron E, et al. The Buffalo Trunk Technique for Aortic Arch Reconstruction. Ann Thorac Surg 2019;108(3):680–686.
57. Yamaguchi D, Jordan WD Jr. Hybrid thoracoabdominal aortic aneurysm repair: current perspectives. Semin Vasc Surg 2012;25(4):203–207.
58. Szeto WY, Bavaria JE. Hybrid repair of aortic arch aneurysms: combined open arch reconstruction and endovascular repair. Semin Thorac Cardiovasc Surg 2009;21(4):347–354.
59. Kouchoukos NT, Masetti P. Total aortic arch replacement with a branched graft and limited circulatory arrest of the brain. J Thorac Cardiovasc Surg 2004;128(2):233–237.

60. Bednarkiewicz M, Khatchatourian G, Christenson JT, Faidutti B. Aortic arch replacement using a four-branched aortic arch graft. Eur J Cardiothorac Surg 2002;21(1):89–91.
61. Spanos K, Panuccio G, Rohlffs F, Heidemann F, Tsilimparis N, Kölbel T. Technical Aspects of Branched Thoracic Arch Graft Implantation for Aortic Arch Pathologies. J Endovasc Ther 2020;27(5):792–800.
62. Sharma VJ, Prakash M, Lin Z, Lo C. What are the endovascular options and outcomes for repair of ascending aortic or aortic arch pathology? Interact Cardiovasc Thorac Surg 2021;32(1):106–110.
63. Burke CR, Kratzberg JA, Yoder AD, Steele NZ, Aldea GS, Sweet MP. Applicability of the Zenith Inner Branched Arch Endograft. J Endovasc Ther 2020;27(2):252–257.
64. Kansagra K, Kang J, Taon MC, et al. Advanced endografting techniques: snorkels, chimneys, periscopes, fenestrations, and branched endografts. Cardiovasc Diagn Ther 2018;8(suppl 1):S175–S183.
65. Wang T, Shu C, Li M, et al. Thoracic Endovascular Aortic Repair With Single/Double Chimney Technique for Aortic Arch Pathologies. J Endovasc Ther 2017;24(3):383–393.
66. Schlösser FJV, Aruny JE, Freiburg CB, Mojibian HR, Sumpio BE, Muhs BE. The chimney procedure is an emergently available endovascular solution for visceral aortic aneurysm rupture. J Vasc Surg 2011;53(5):1386–1390.
67. Kuzniar MK, Wanhainen A, Tegler G, Mani K. Endovascular treatment of chronic aortic dissection with fenestrated and branched stent-grafts. J Vasc Surg 2021;73(5):1573–1582.
68. LeMaire SA, Carter SA, Coselli JS. The elephant trunk technique for staged repair of complex aneurysms of the entire thoracic aorta. Ann Thorac Surg 2006;81(5):1561–1569; discussion 1569.
69. Johnson PT, Corl FM, Black JH, Fishman EK. The elephant trunk procedure for aortic aneurysm repair: an illustrated guide to surgical technique with CT correlation. AJR Am J Roentgenol 2011;197(6):W1052–W1059.
70. Kreibich M, Siepe M, Berger T, et al. The Frozen Elephant Trunk Technique for the Treatment of Type B and Type Non-A Non-B Aortic Dissection. Eur J Vasc Endovasc Surg 2021;61(1):107–113.
71. Song SB, Wu XJ, Sun Y, Cai SH, Hu PY, Qiang HF. A modified frozen elephant trunk technique for acute Stanford type A aortic dissection. J Cardiothorac Surg 2020;15(1):322.
72. Karck M, Chavan A, Hagl C, Friedrich H, Galanski M, Haverich A. The frozen elephant trunk technique: a new treatment for thoracic aortic aneurysms. J Thorac Cardiovasc Surg 2003;125(6):1550–1553.